AST-121: Galactic Astronomy

(but really, stellar structure and evolution)

http://cosmos.phy.tufts.edu/~danilo/AST121/AST121.html

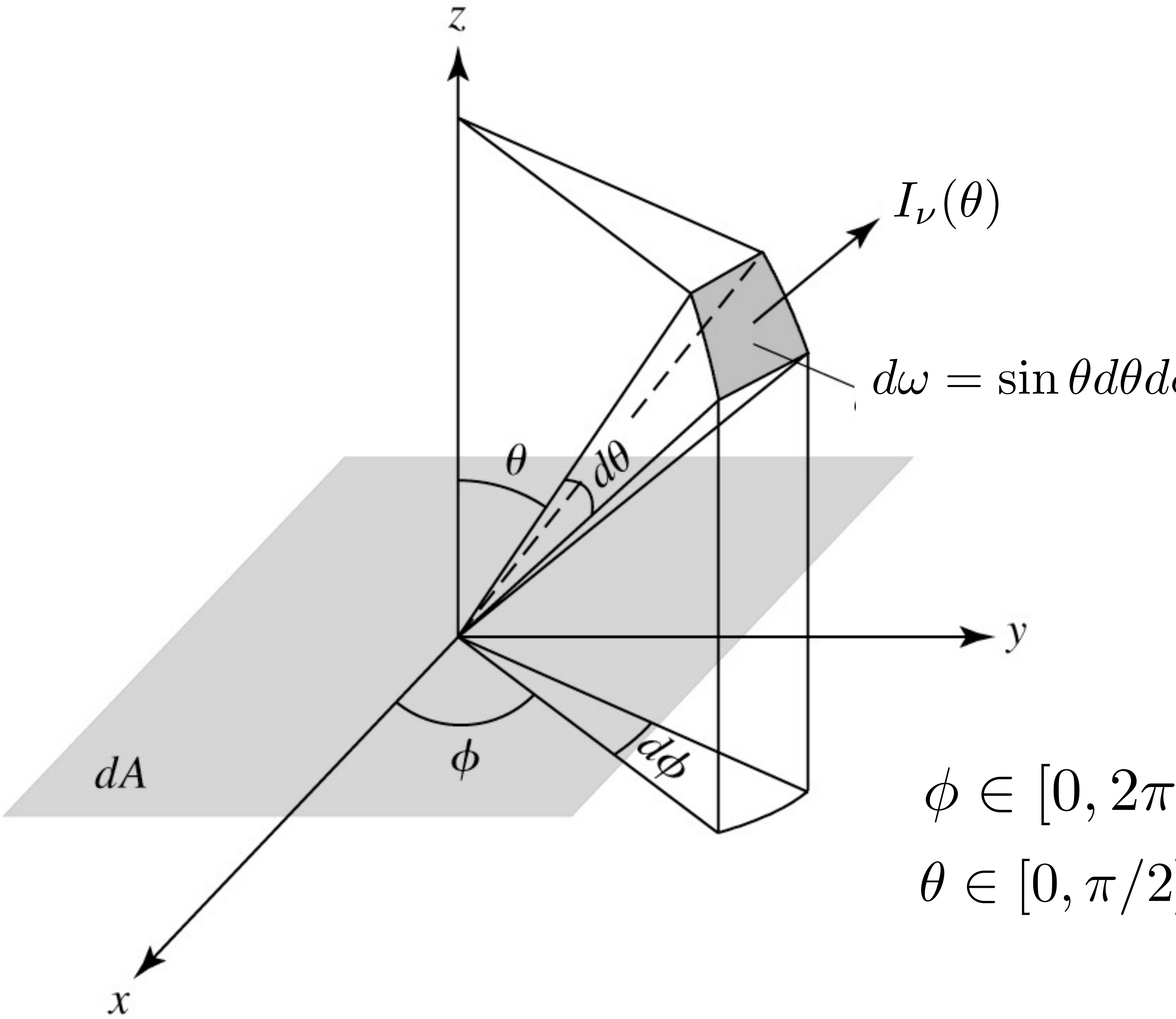

$$\phi \in [0, 2\pi]$$

$$\theta \in [0, \pi/2]$$

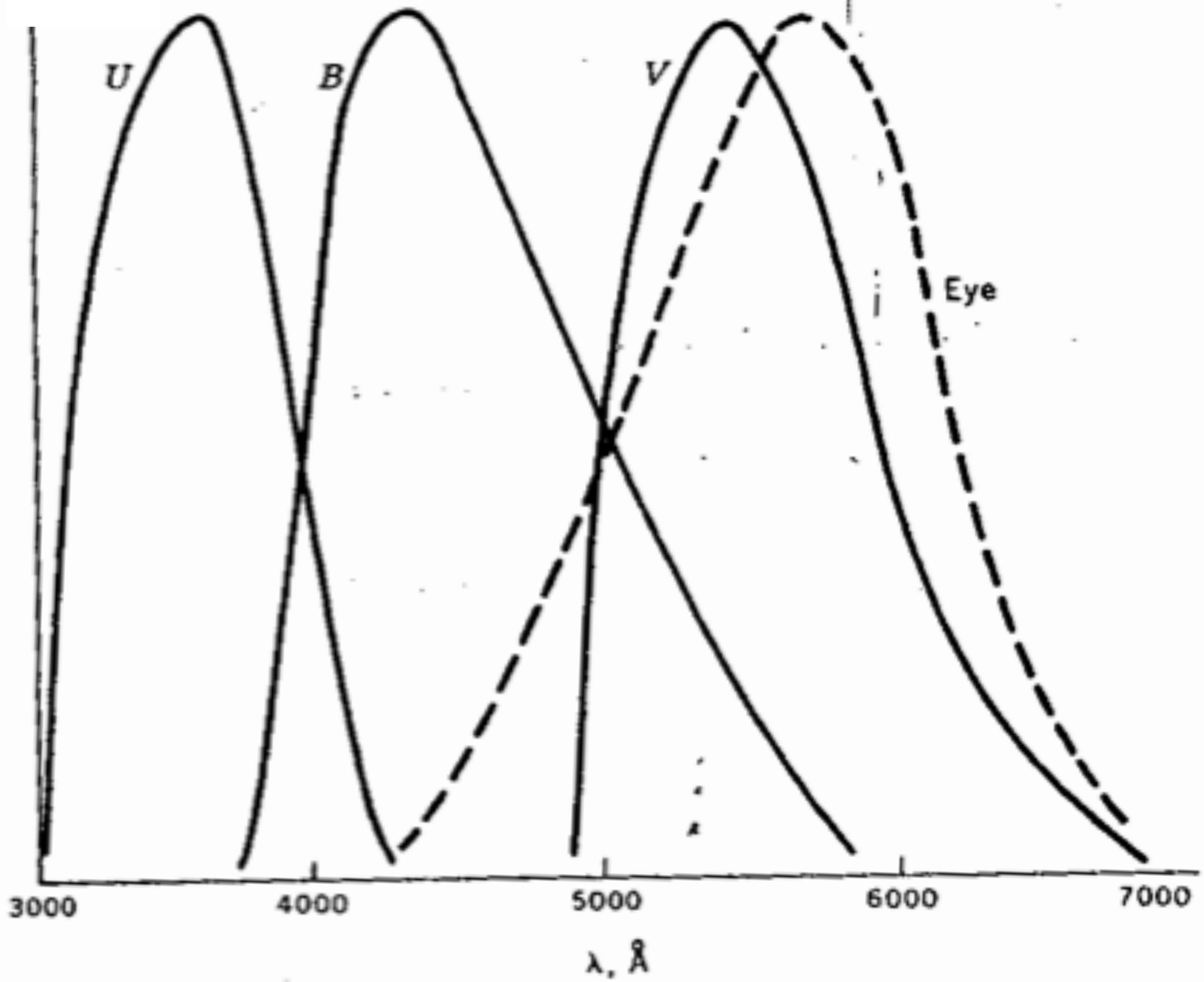

Fig. 1-6 A schematic comparison of the spectral responses of the *U*, *B*, and *V* detector systems used in multicolor photometry. The response of the human eye is shown for comparison.

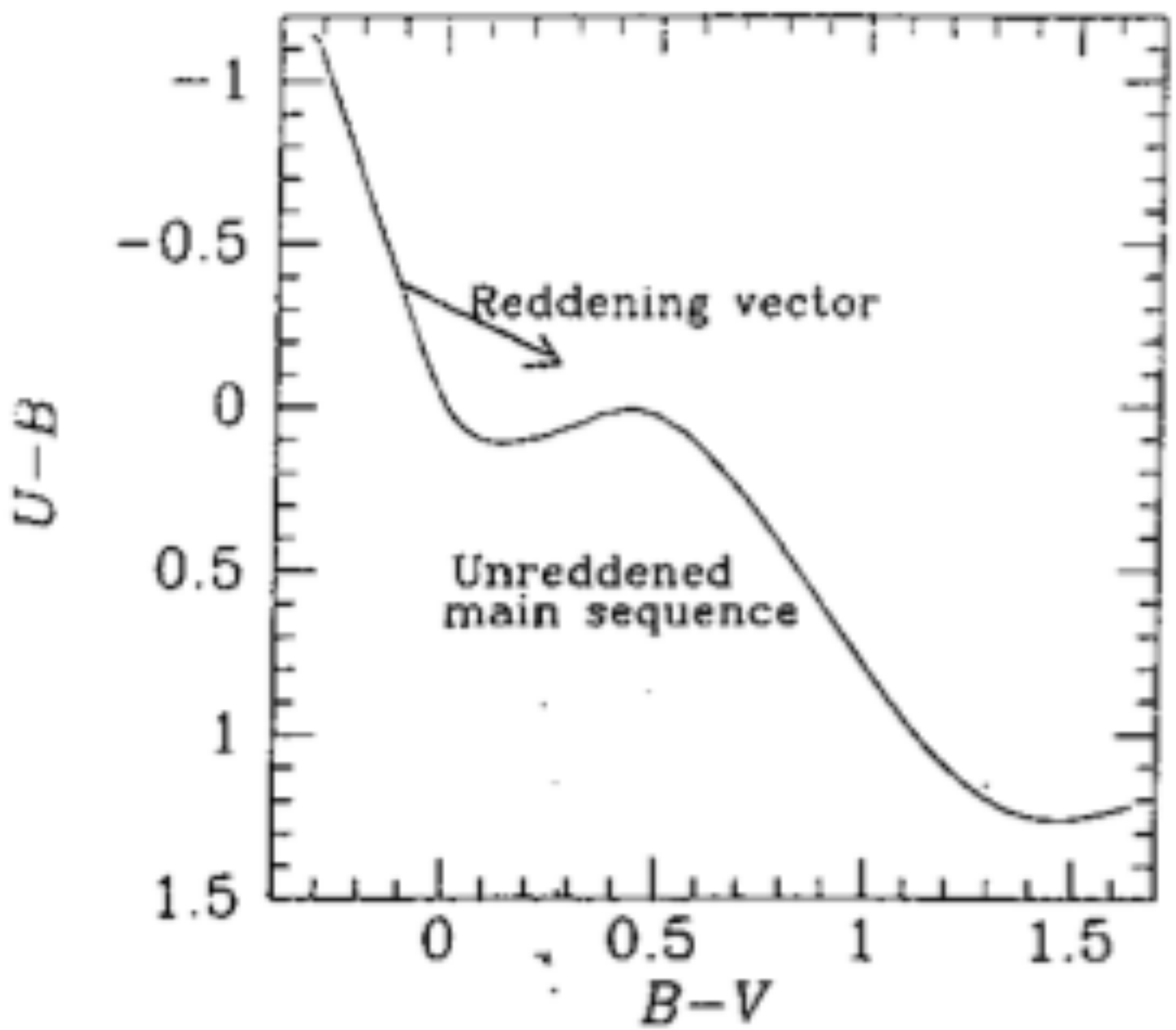

Figure 3.16 Effects of interstellar reddening in the *UBV*-system two-color diagram.

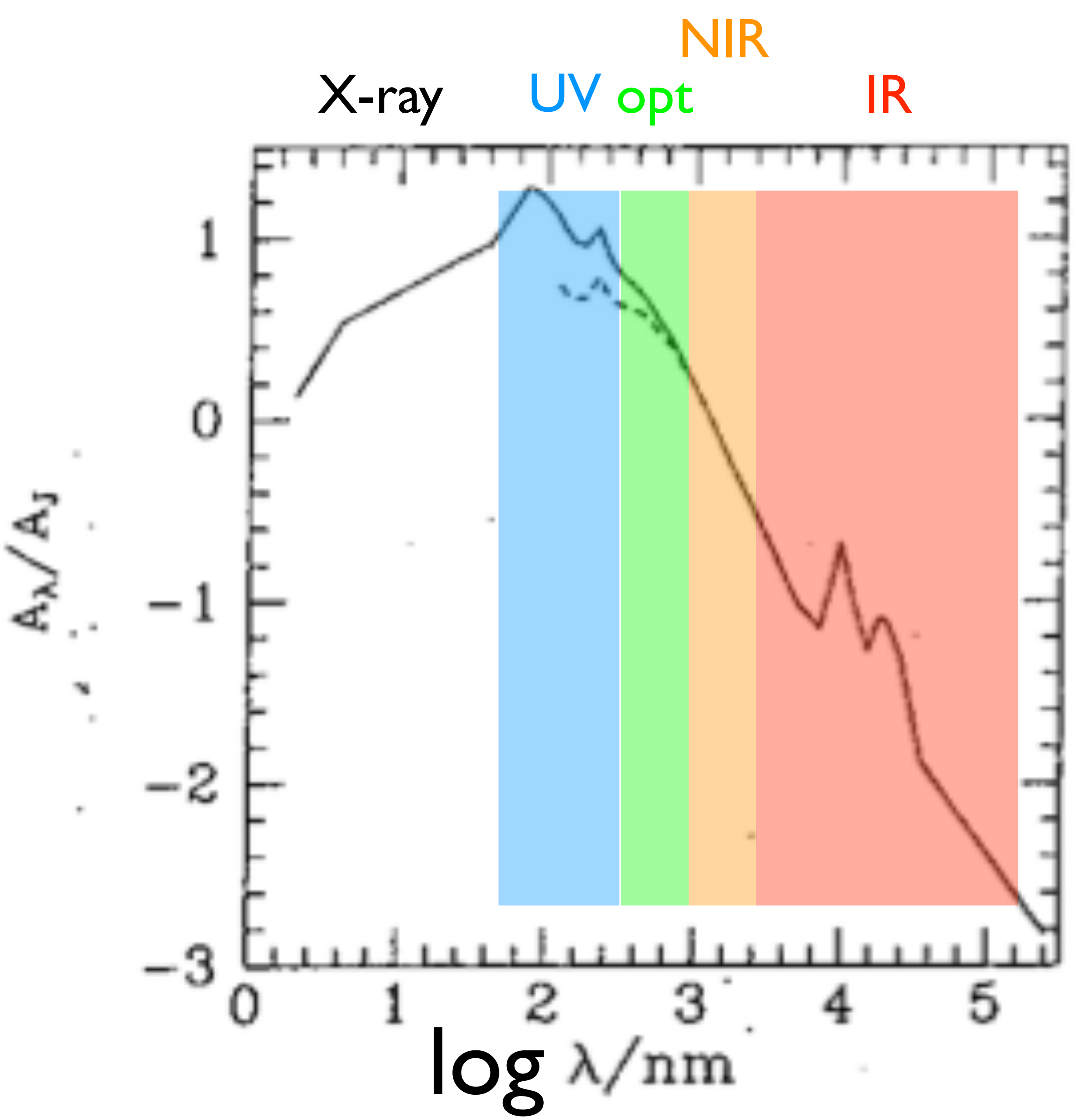

Figure 3.17 The interstellar extinction curve for two representative lines of sight. The full curve is characteristic of lines of sight that pass only through the intercloud medium, while the dashed curve is for a line of sight that penetrates deep into a molecular cloud. [From data published in Mathis (1990)]

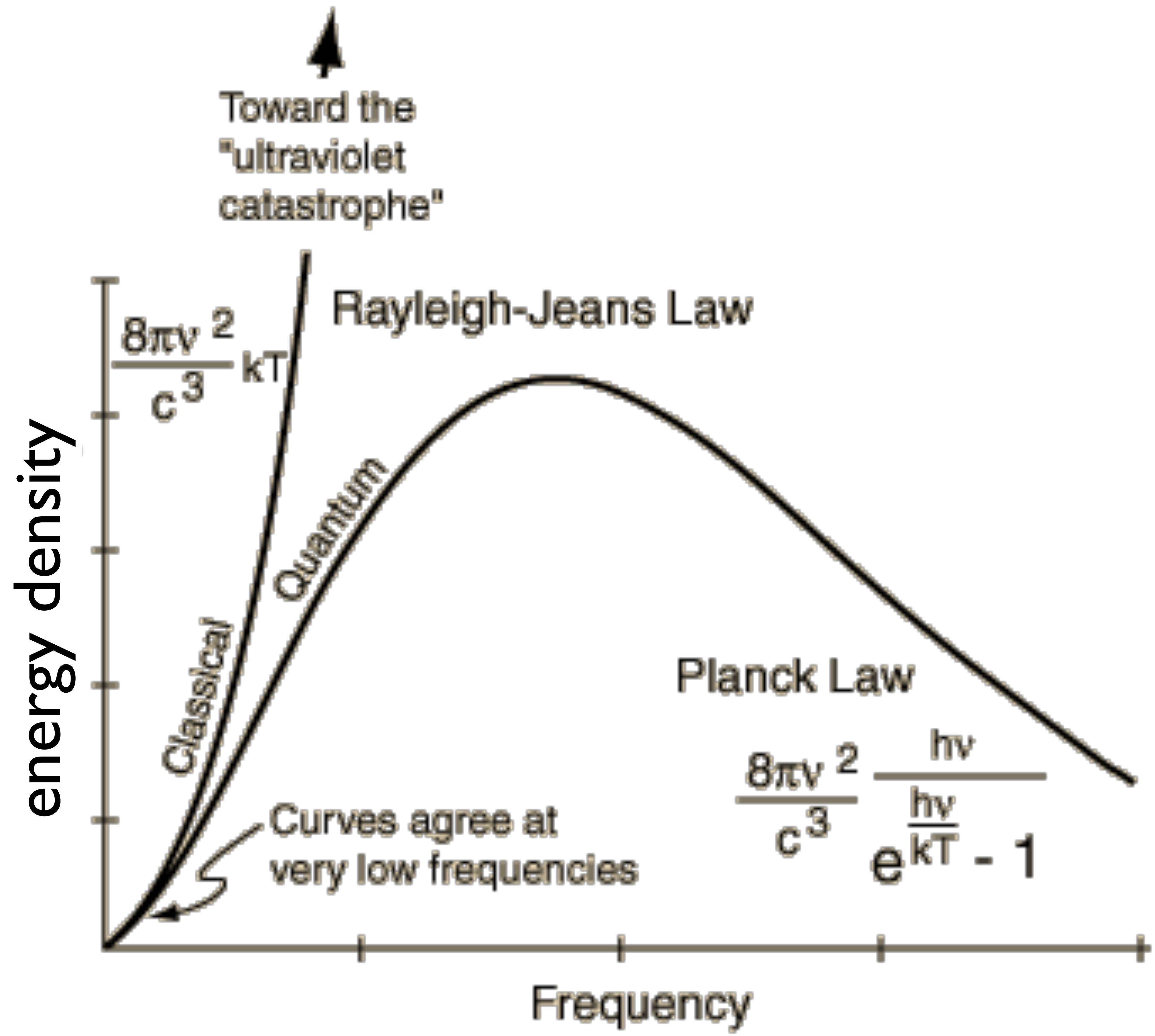

Toward the "ultraviolet catastrophe"
Rayleigh-Jeans Law
$\frac{8\pi\nu^2}{c^3}kT$
Classical
Quantum
Planck Law
$\frac{8\pi\nu^2}{c^3}\frac{h\nu}{e^{\frac{h\nu}{kT}}-1}$
Curves agree at very low frequencies
energy density
Frequency

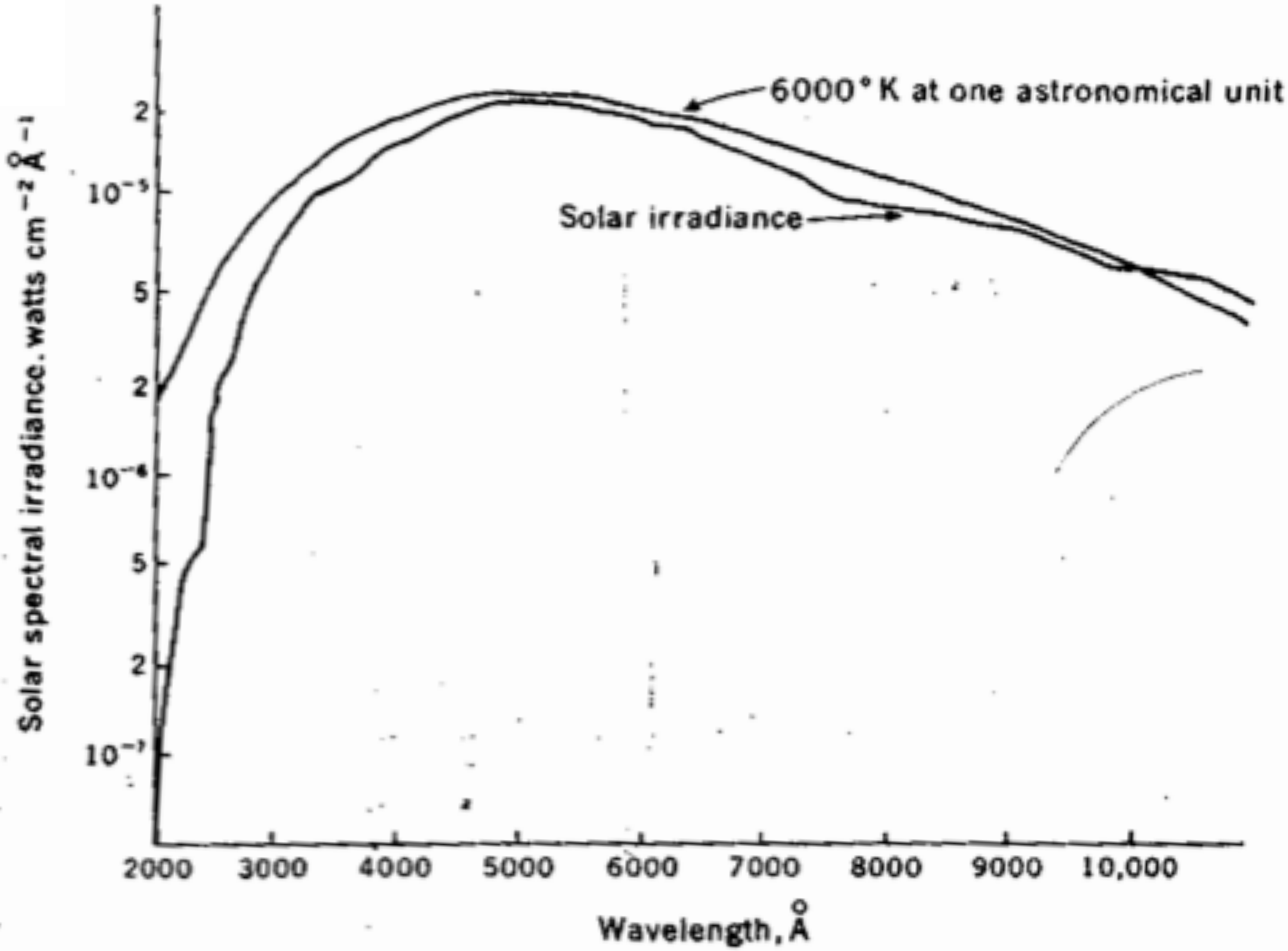

Fig. 1-5 Comparison of the visible solar energy-distribution curve with that from a blackbody at 6000°K. The overall resemblance is good, although the sun is quite deficient in the ultraviolet. [*D. P. Le Galley and A. Rosen (eds.), "Space Physics," p.* 111, *John Wiley & Sons, Inc., New York*, 1964.]

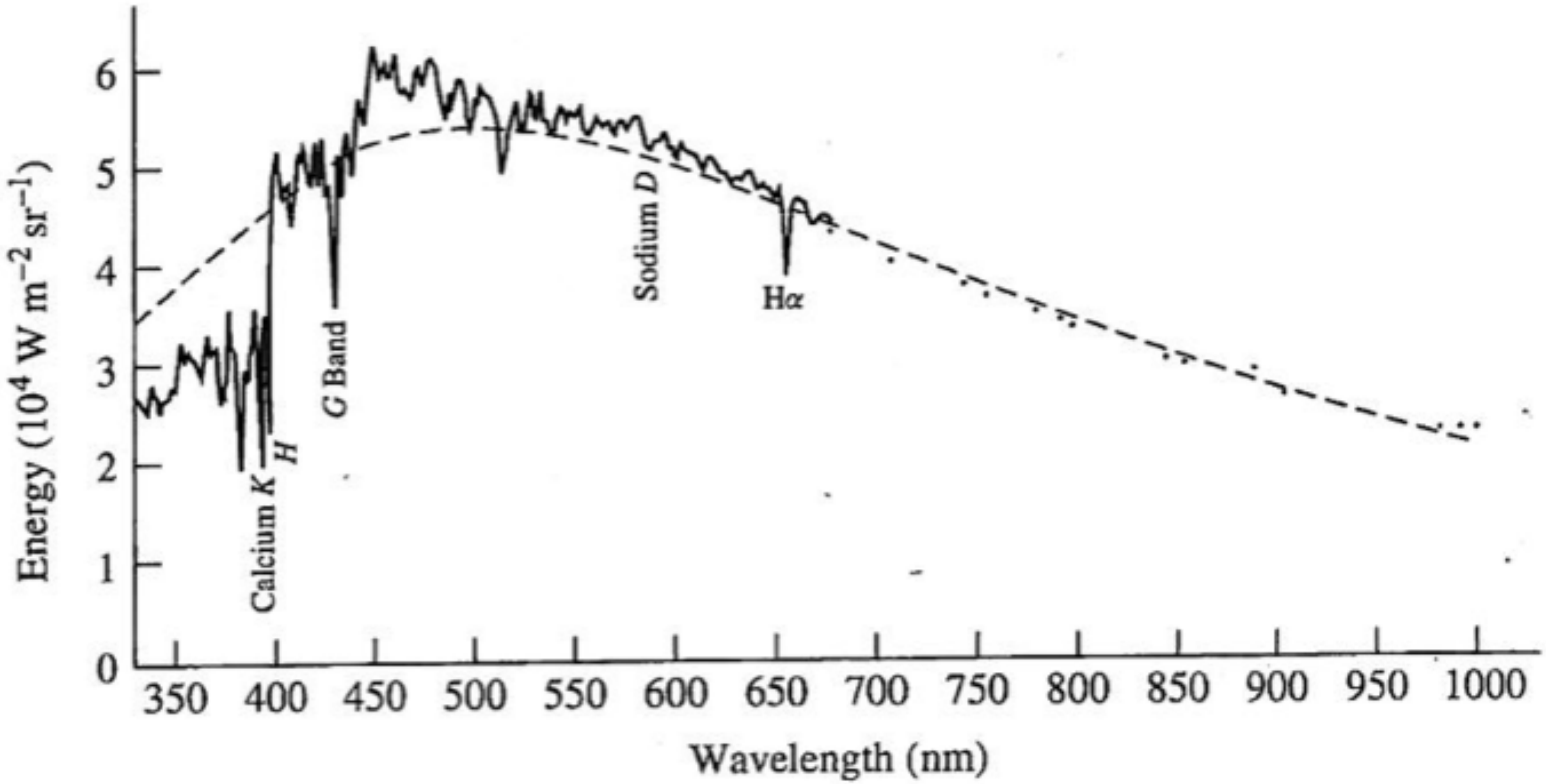

FIGURE 9.5 The spectrum of the Sun in 2 nm wavelength intervals. The dashed line is the curve of an ideal blackbody having the Sun's effective temperature. (Figure adapted from Aller, *Atoms, Stars, and Nebulae*, Third Edition, Cambridge University Press, New York, 1991.)

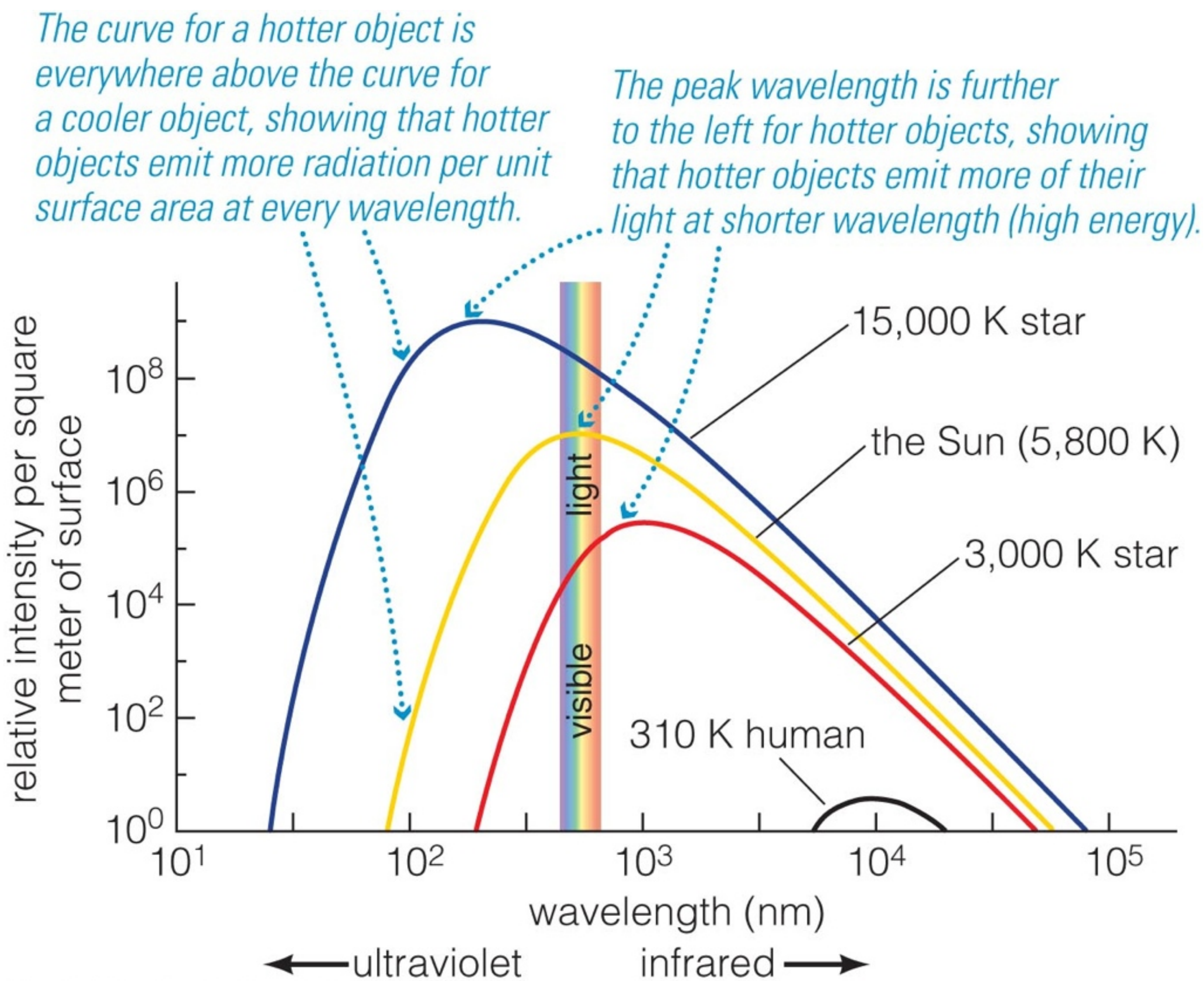
The curve for a hotter object is everywhere above the curve for a cooler object, showing that hotter objects emit more radiation per unit surface area at every wavelength.
The peak wavelength is further to the left for hotter objects, showing that hotter objects emit more of their light at shorter wavelength (high energy).
15,000 K star
the Sun (5,800 K)
3,000 K star
310 K human
visible light
relative intensity per square meter of surface
wavelength (nm)
ultraviolet
infrared

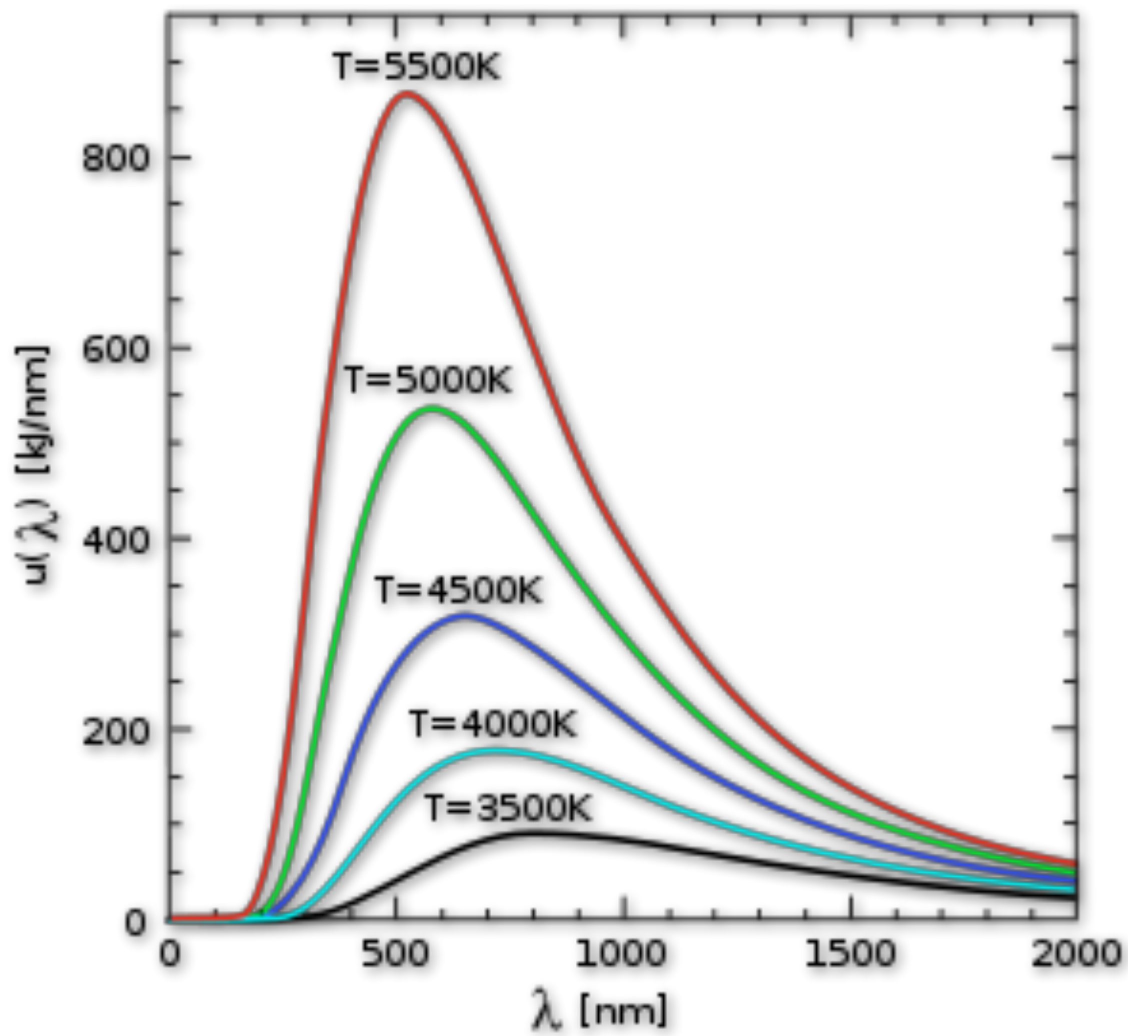
T=5500K
T=5000K
T=4500K
T=4000K
T=3500K
u(λ) [kJ/nm]
λ [nm]

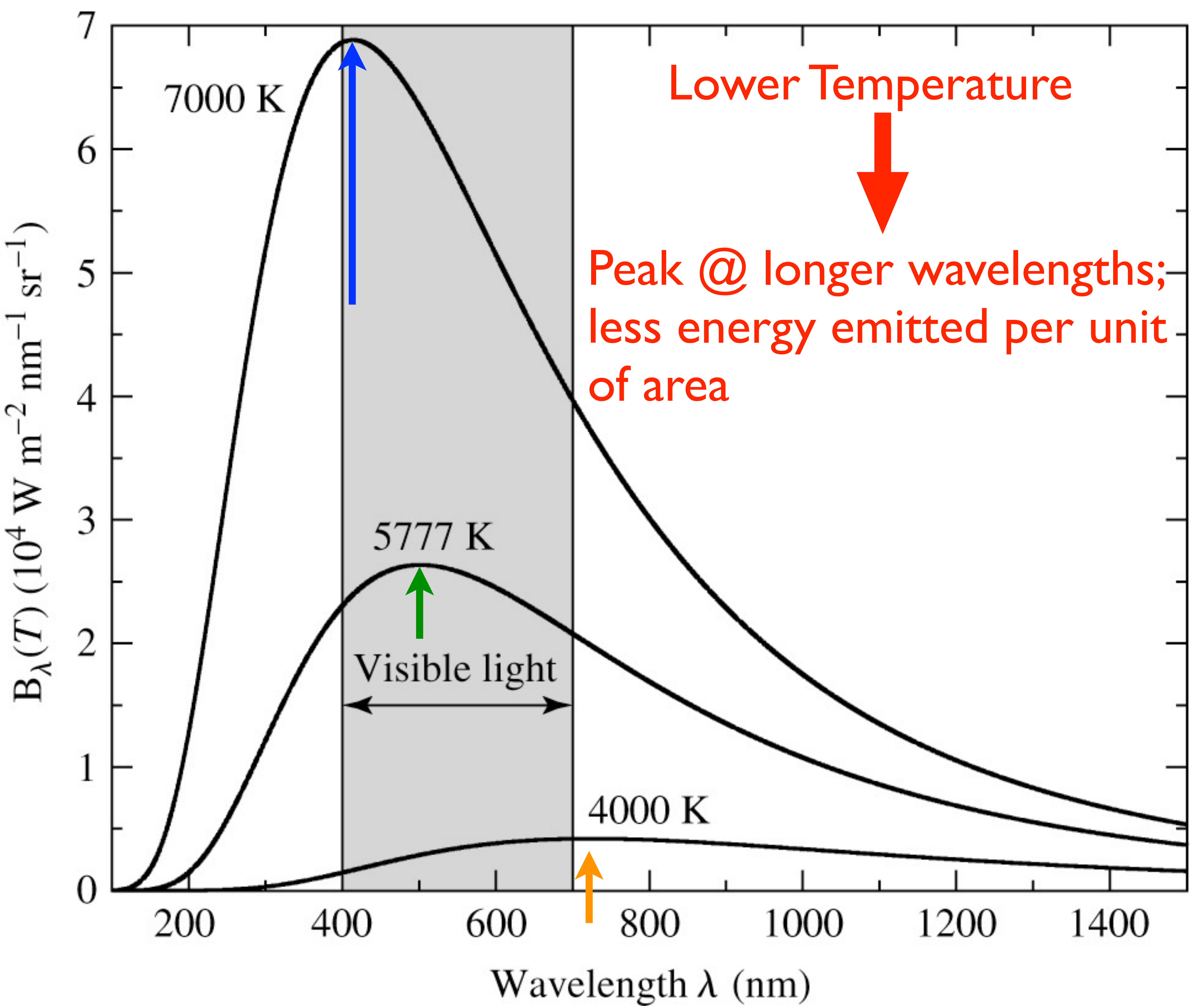

7000 K
5777 K
4000 K
Visible light
Lower Temperature
Peak @ longer wavelengths; less energy emitted per unit of area
$B_\lambda(T)$ (10^4 W m^{-2} nm^{-1} sr^{-1})
Wavelength λ (nm)
0
1
2
3
4
5
6
7
200
400
600
800
1000
1200
1400

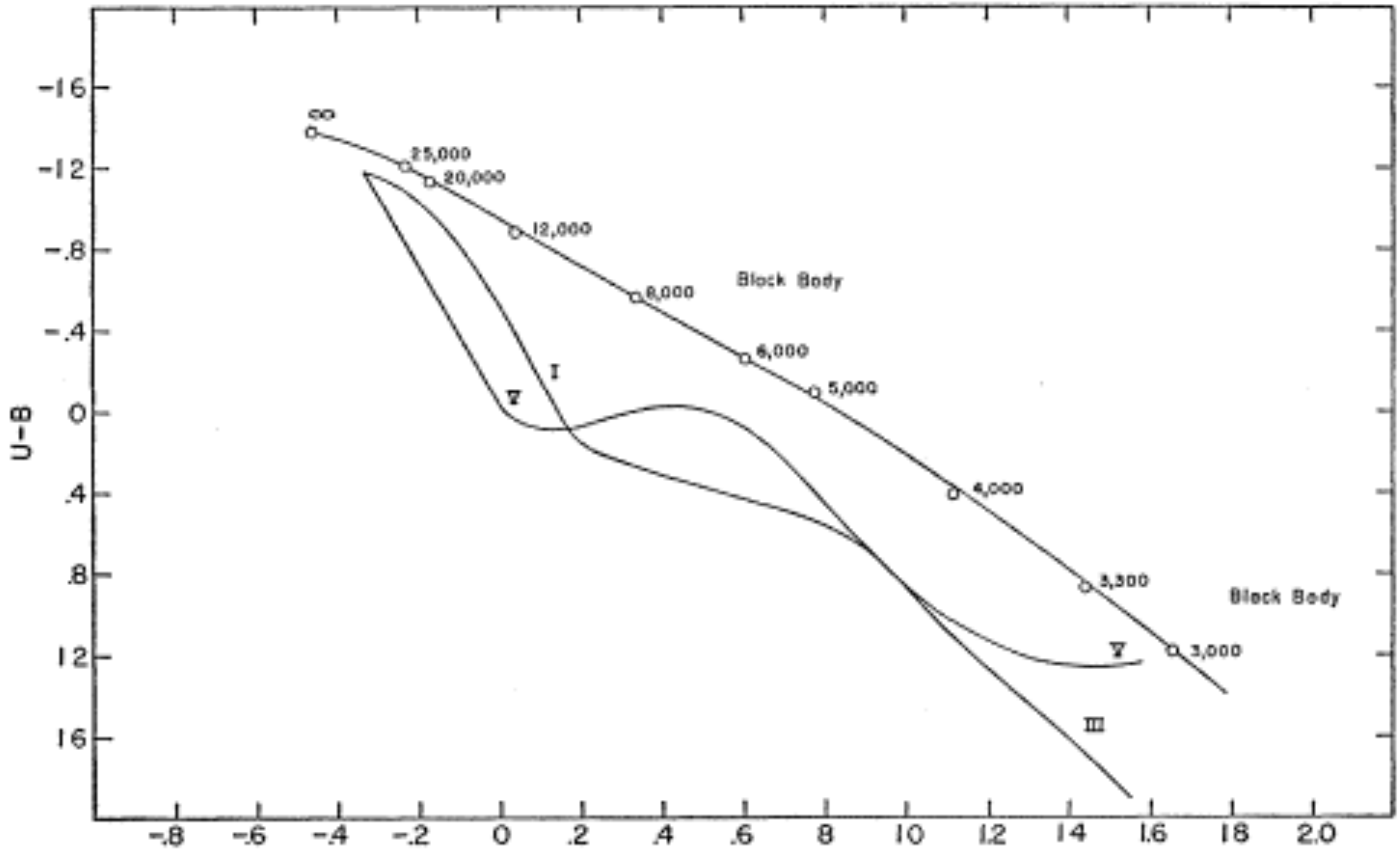

FIG. 1.—The $U - B$, $B - V$ relation for black bodies. The plotted points are taken from the last two columns of Table 2. The standard Johnson relations for stars of luminosity classes I–V are also shown.

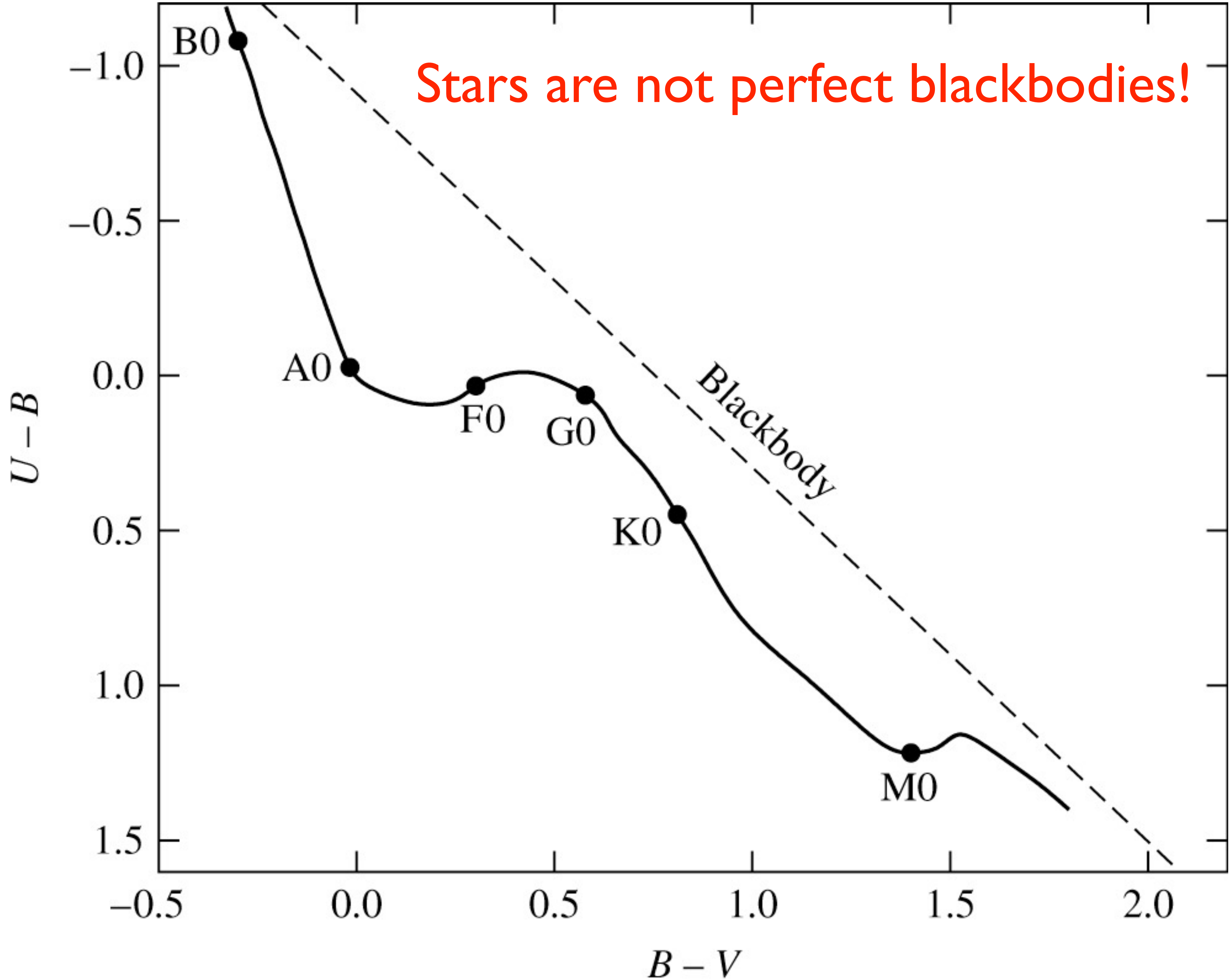

Stars are not perfect blackbodies!
B0
A0
F0
G0
K0
M0
Blackbody
−1.0
−0.5
0.0
0.5
1.0
1.5
U − B
−0.5
0.0
0.5
1.0
1.5
2.0
B − V

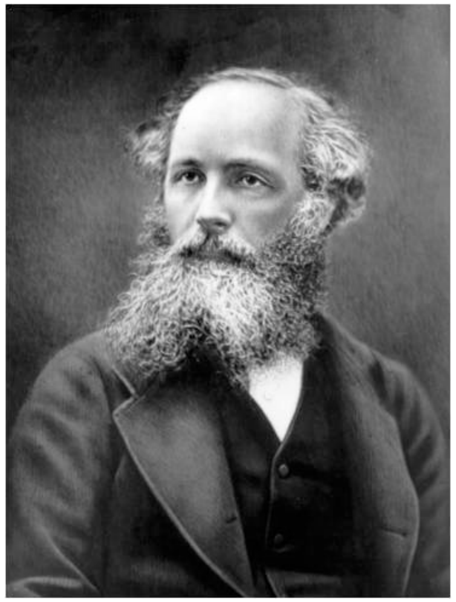

MAXWELL-BOLTZMANN EQ.

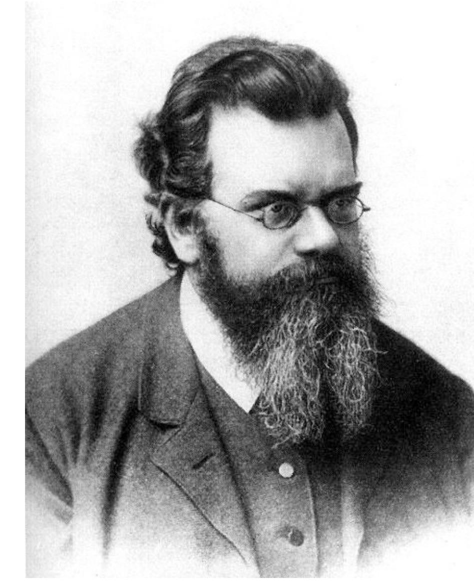

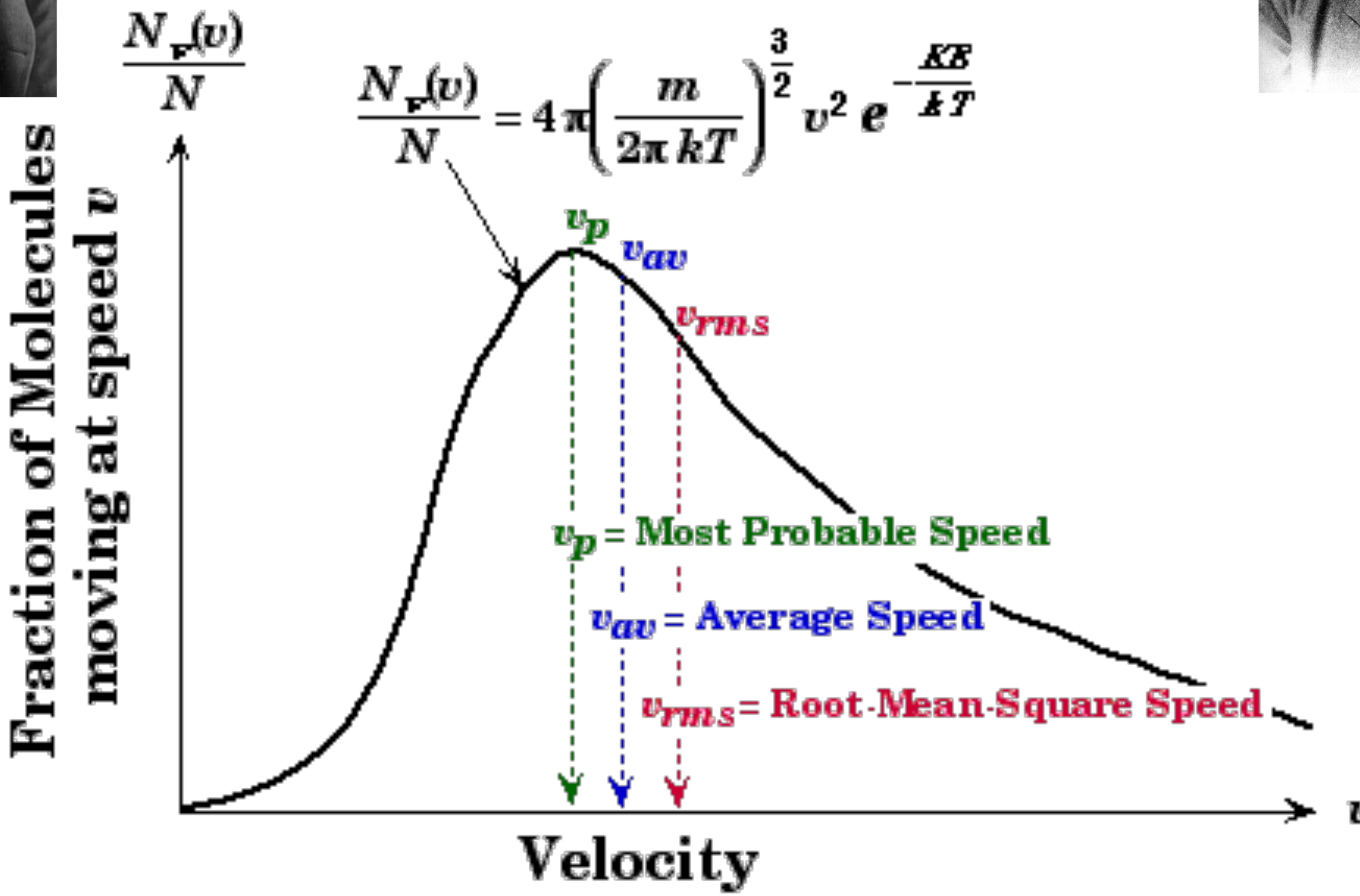

$$v_p = \sqrt{2\frac{kT}{m}} \qquad v_{av} = \sqrt{\frac{8}{\pi}\frac{kT}{m}} \qquad v_{rms} = \sqrt{3\frac{kT}{m}}$$

Maxwell-Boltzmann velocity distribution

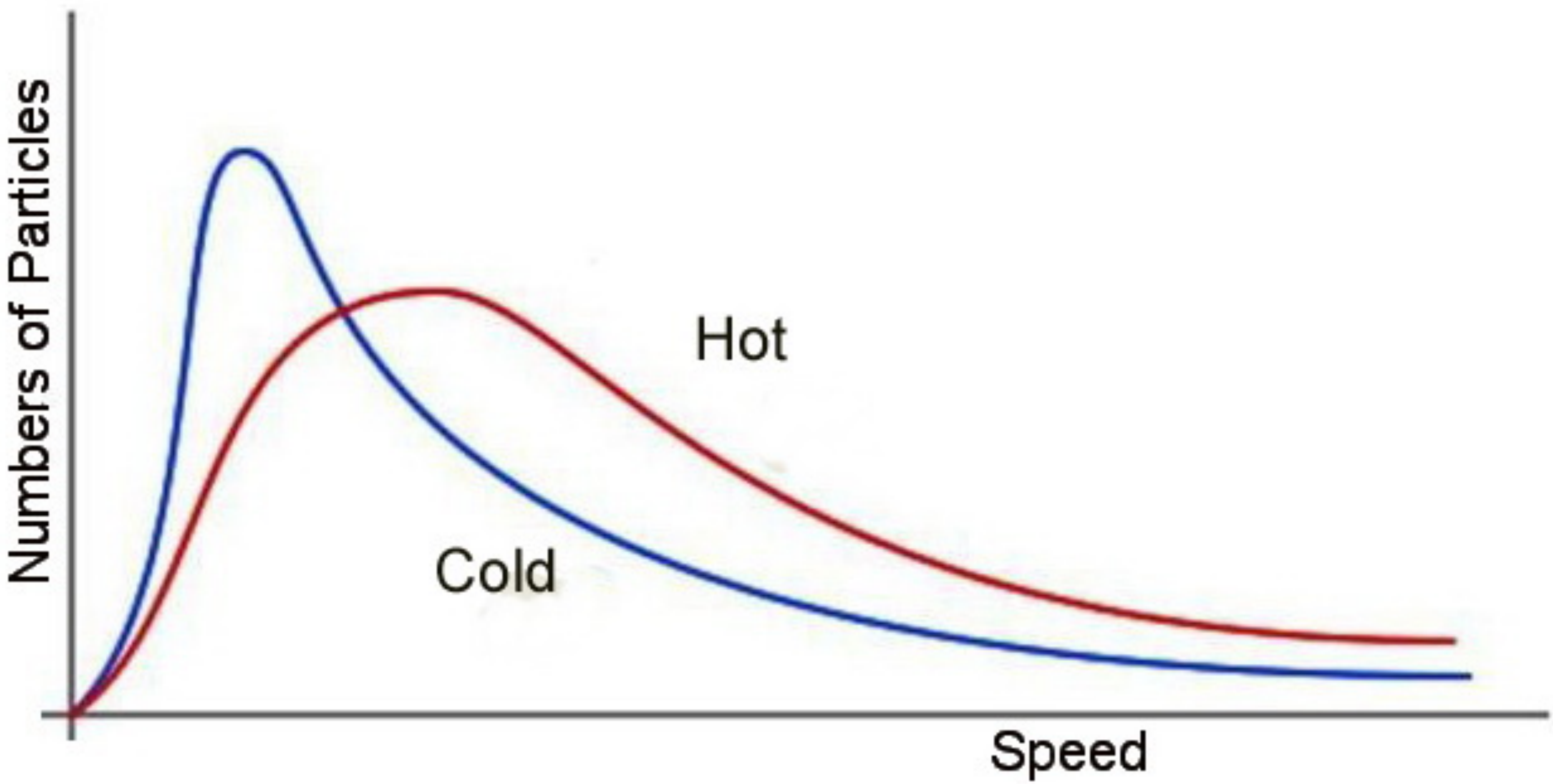

MAXWELL-BOLTZMANN EQ.

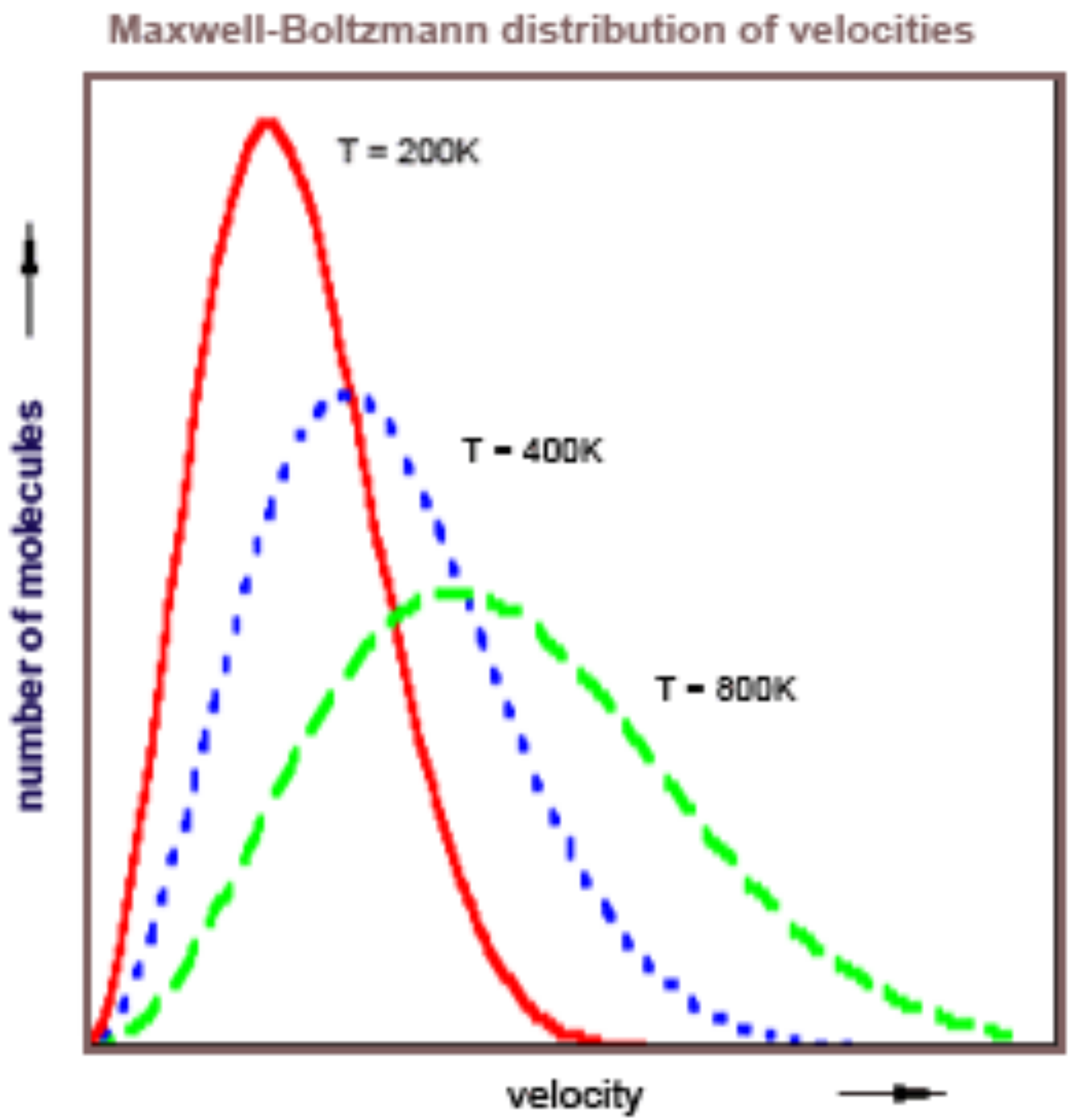

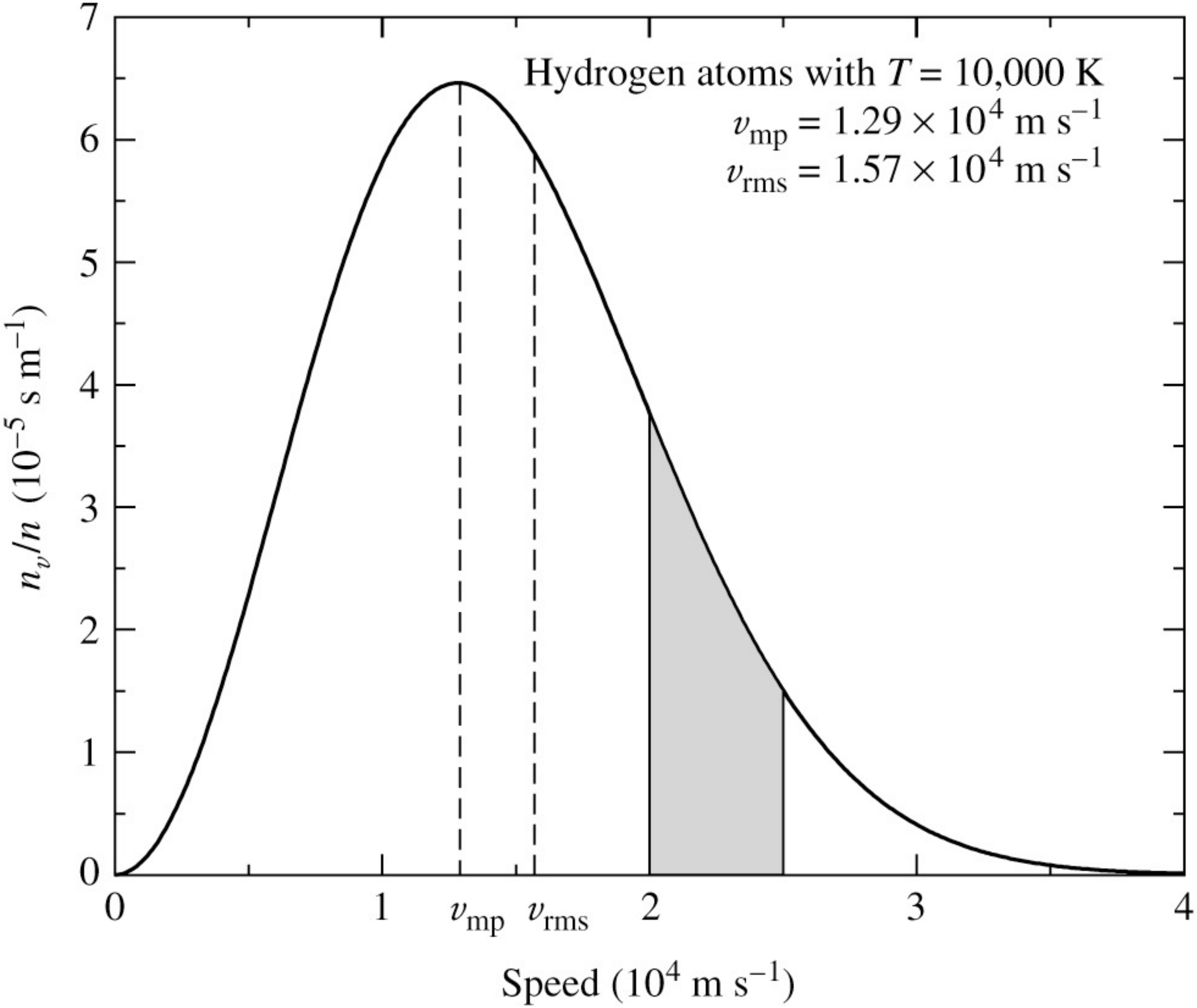

Hydrogen atoms with T = 10,000 K
$v_{mp} = 1.29 \times 10^4$ m s^{-1}
$v_{rms} = 1.57 \times 10^4$ m s^{-1}
n_v/n (10^{-5} s m^{-1})
0
1
2
3
4
5
6
7
0
1
v_{mp}
v_{rms}
2
3
4
Speed (10^4 m s^{-1})

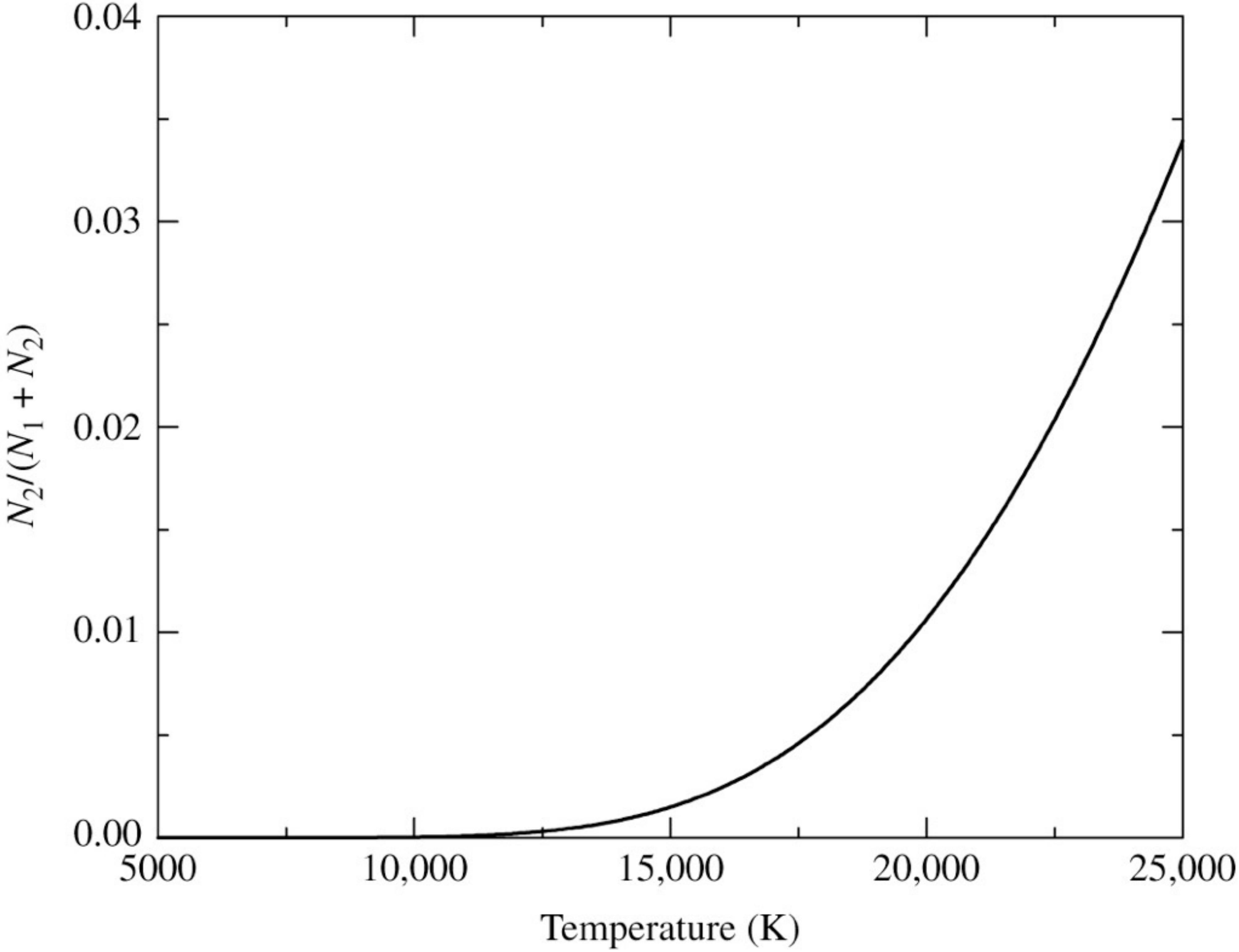
0.04
0.03
0.02
0.01
0.00
5000
10,000
15,000
20,000
25,000
Temperature (K)
$N_2/(N_1 + N_2)$

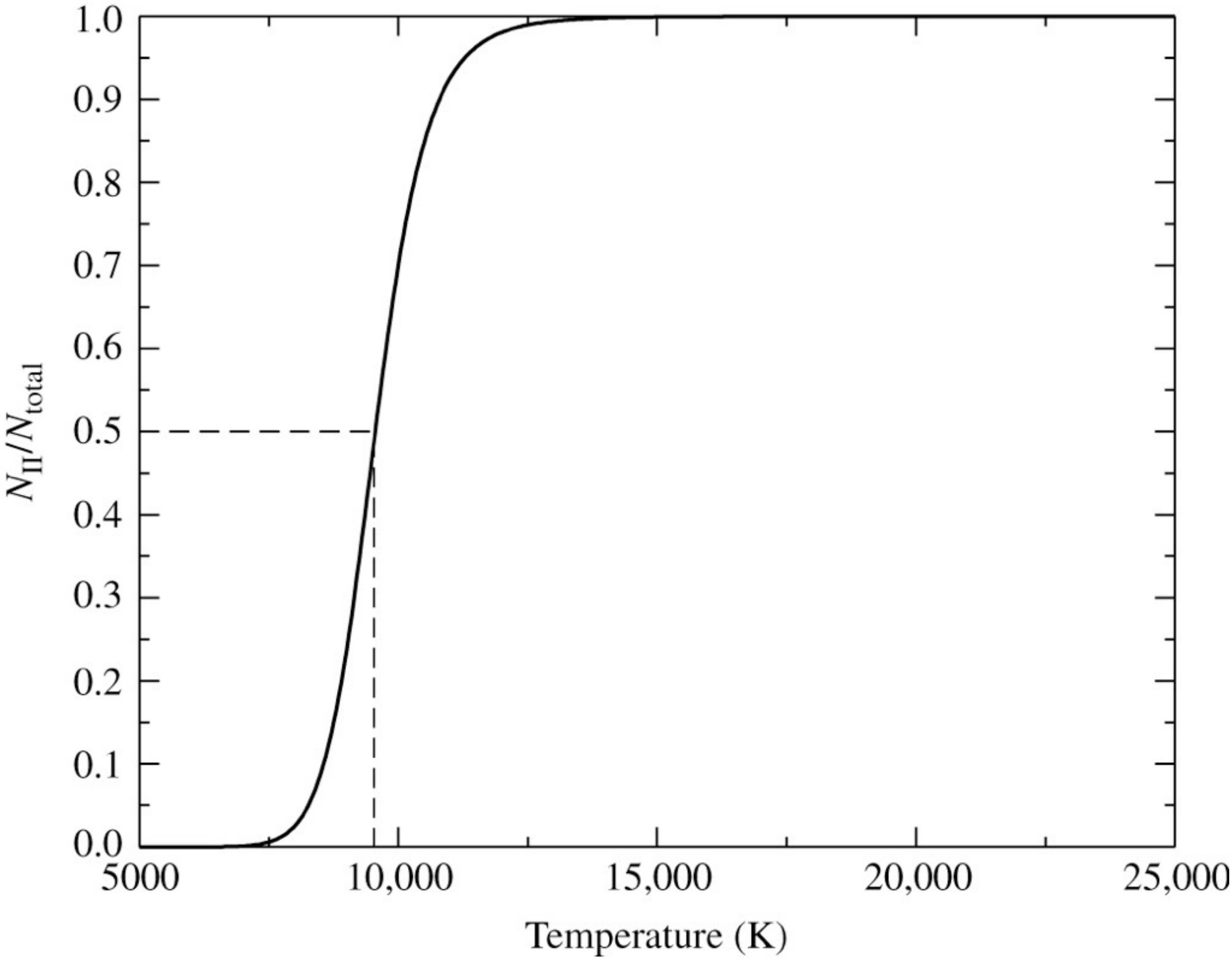

1.0
0.9
0.8
0.7
0.6
0.5
0.4
0.3
0.2
0.1
0.0
N_{II}/N_{total}
5000
10,000
15,000
20,000
25,000
Temperature (K)

Combining Boltzmann eq. with Saha's eq.

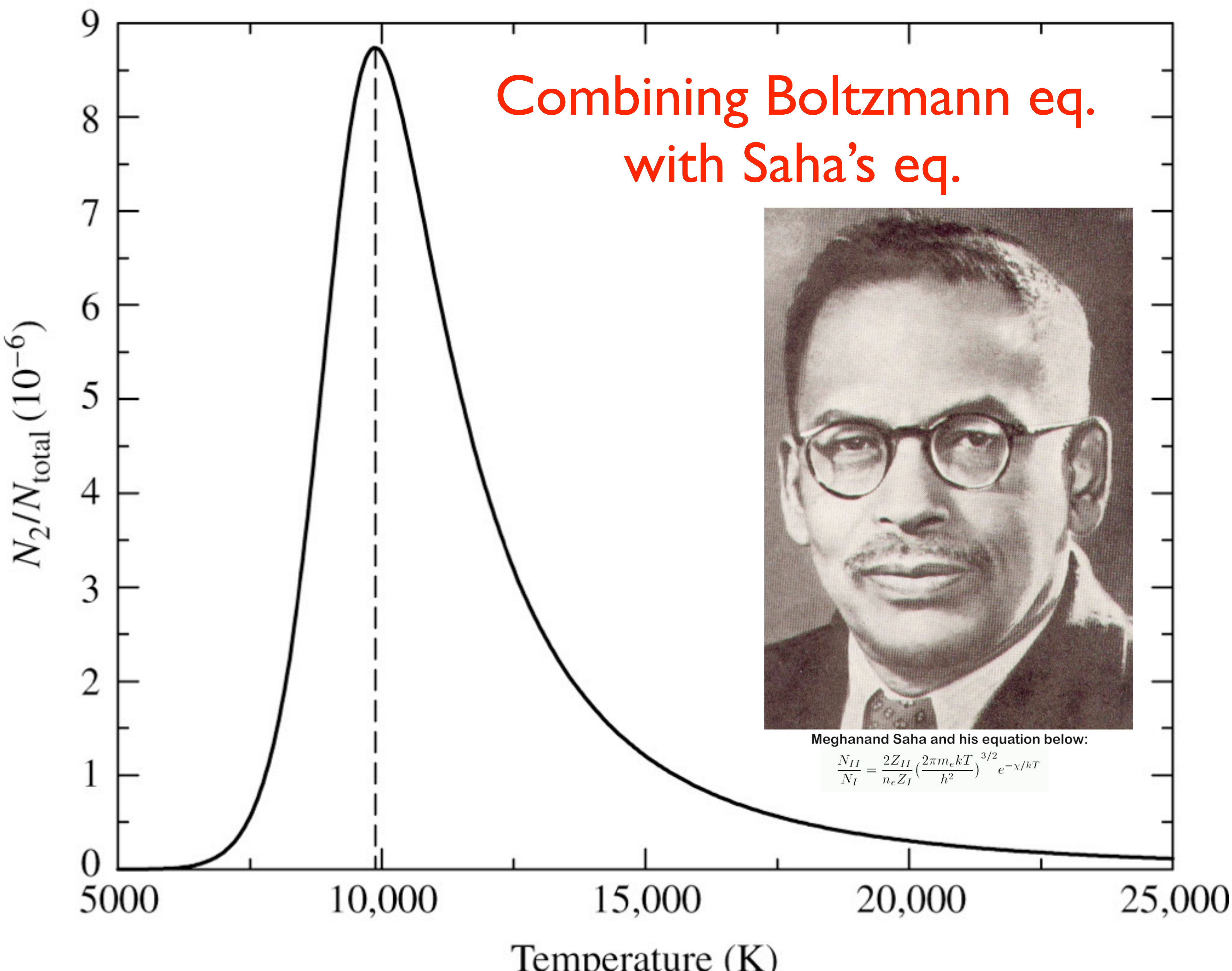

Meghanand Saha and his equation below:

$$\frac{N_{II}}{N_I} = \frac{2Z_{II}}{n_e Z_I}\left(\frac{2\pi m_e kT}{h^2}\right)^{3/2} e^{-\chi/kT}$$

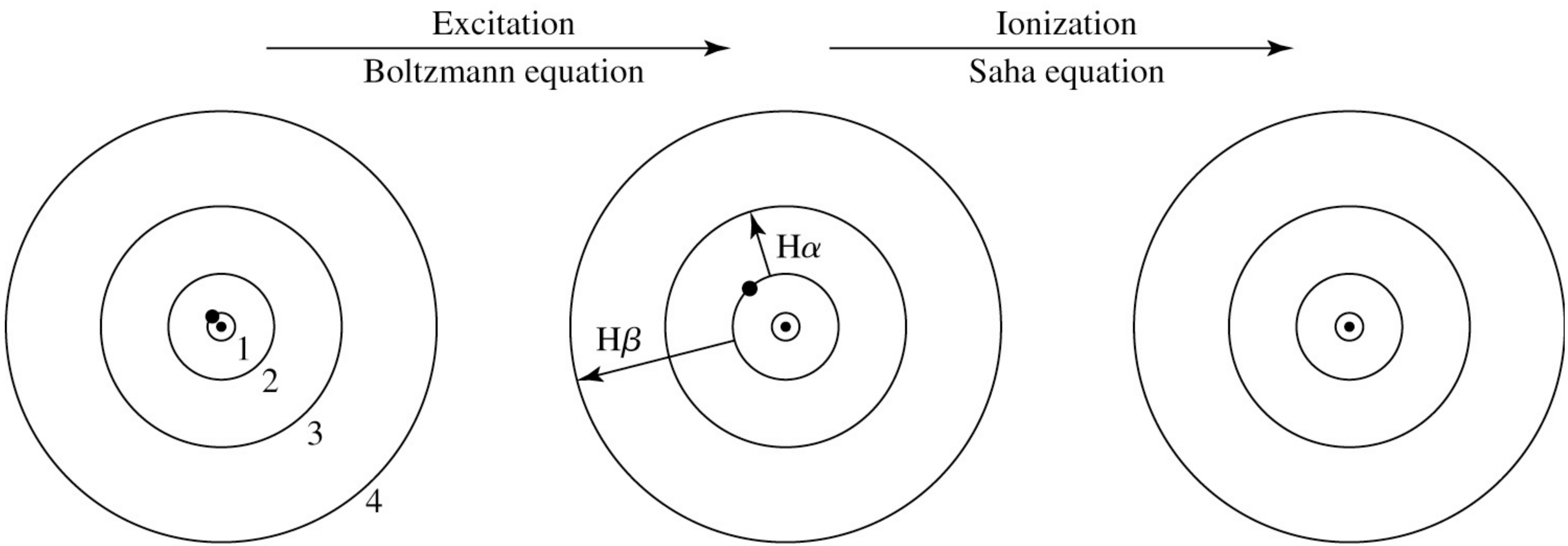

(a) $T < 9900$ K

(b) $T = 9900$ K

(c) $T > 9900$ K

All electrons on ground energy level, hence none are on the 1st excited level to make upper transitions => no Balmer lines

Temperature is right for significant electrons to be excited on the 1st excited level => Balmer lines

Temperature is so large, Hydrogen atoms are ionized, so no electrons => no Balmer lines

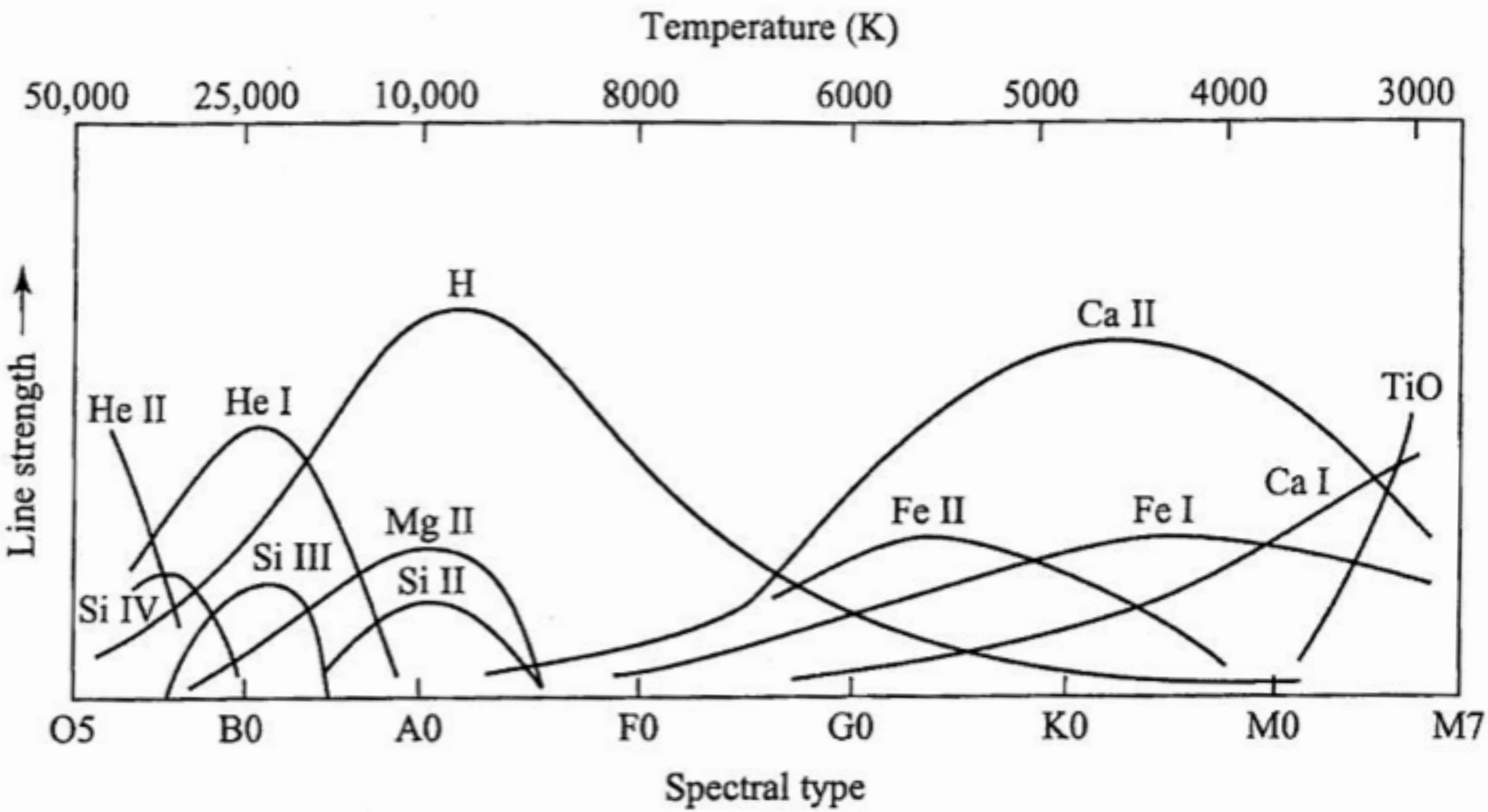

FIGURE 8.11 The dependence of spectral line strengths on temperature.

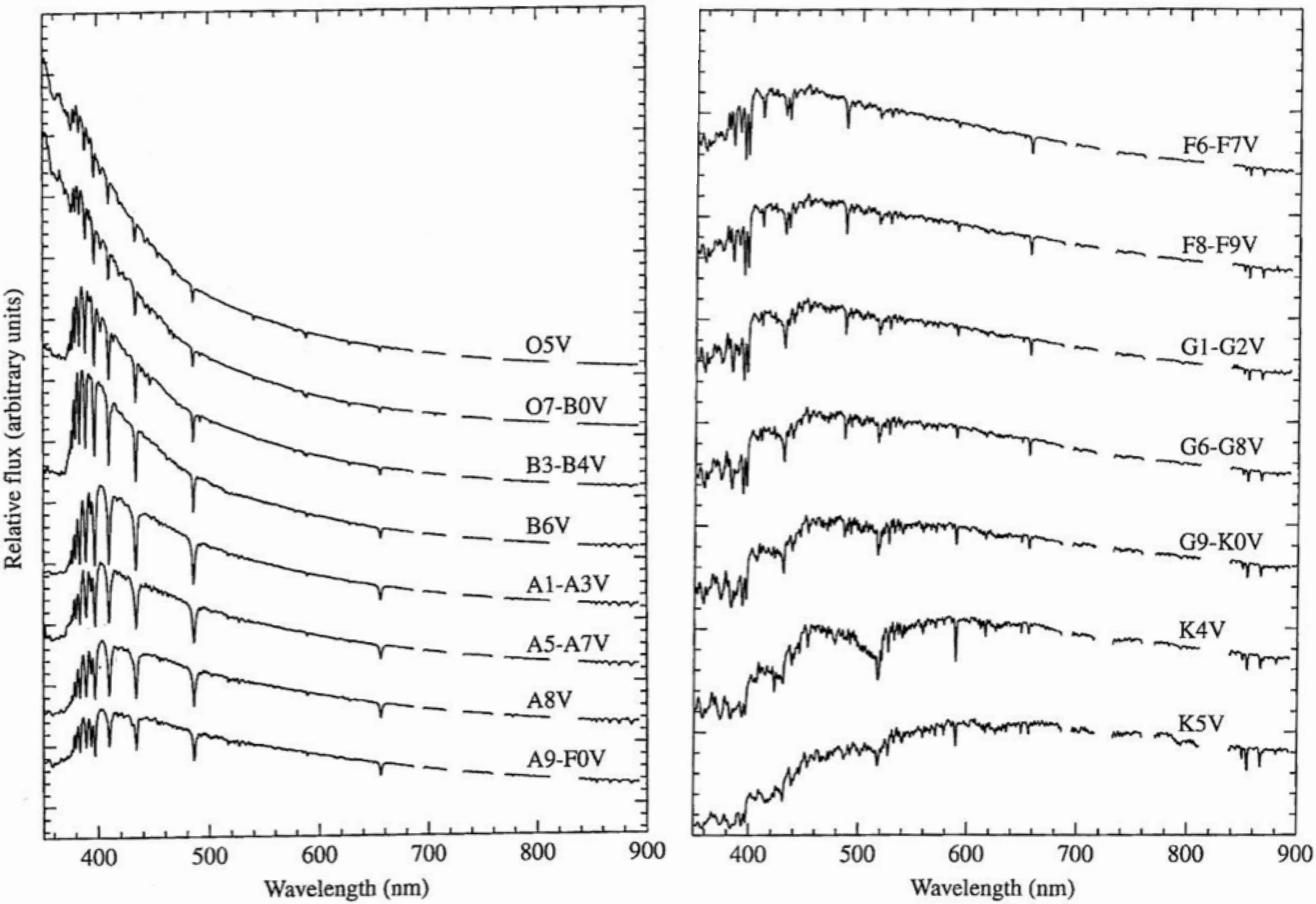

Relative flux (arbitrary units)
O5V
O7-B0V
B3-B4V
B6V
A1-A3V
A5-A7V
A8V
A9-F0V
F6-F7V
F8-F9V
G1-G2V
G6-G8V
G9-K0V
K4V
K5V
400
500
600
700
800
900
Wavelength (nm)
400
500
600
700
800
900
Wavelength (nm)

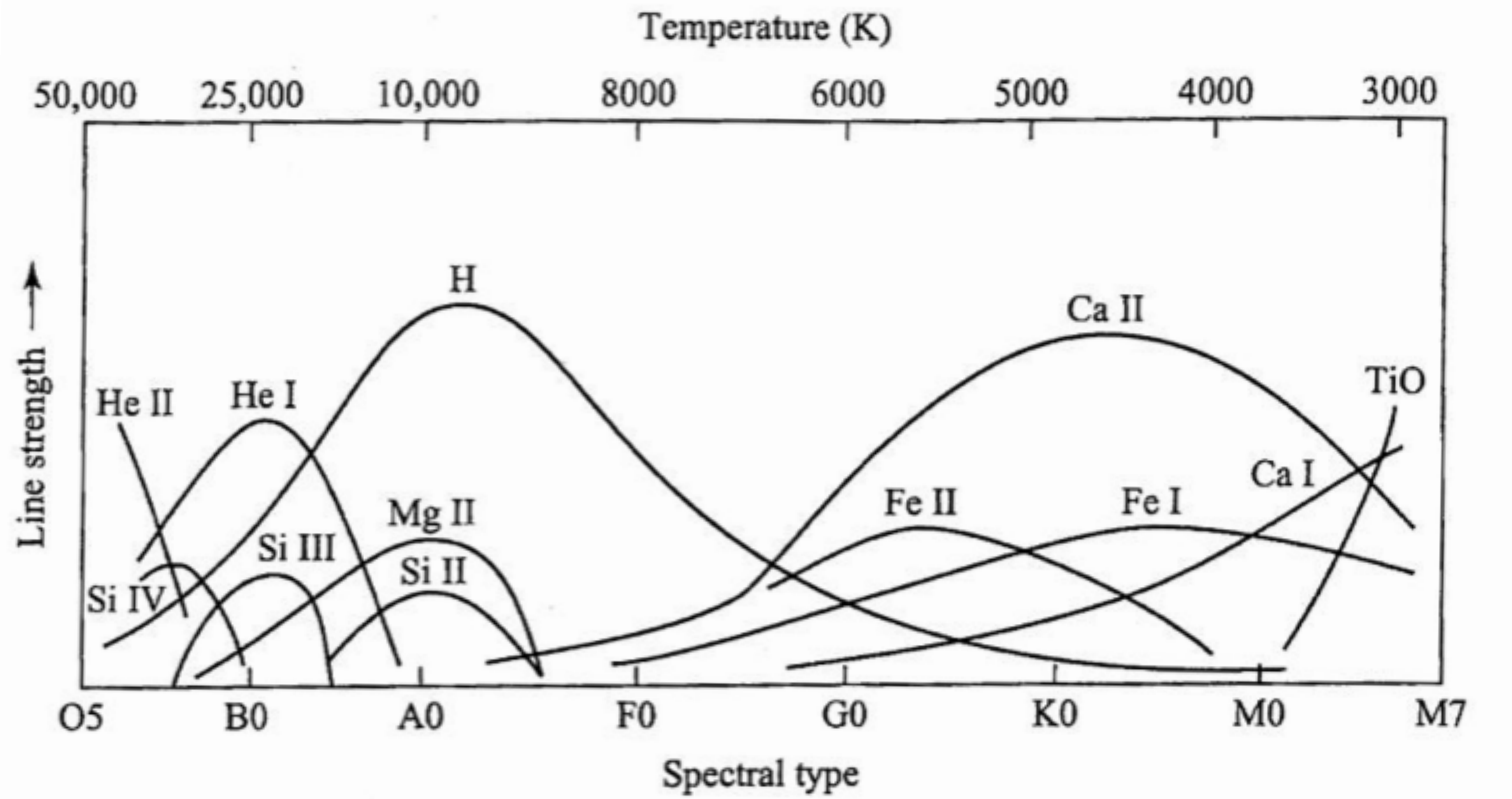

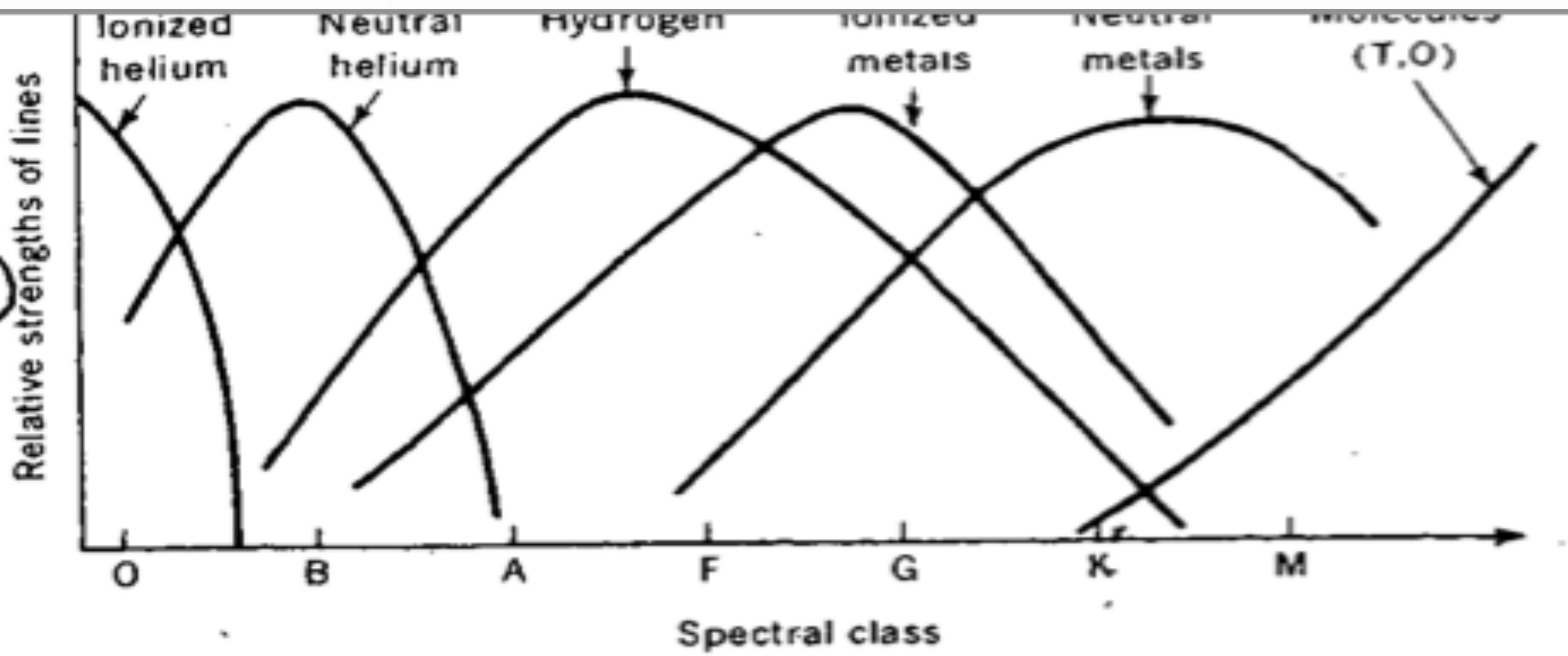

Fig. 1-11 The progression of selected spectral properties through the sequence of spectral classes. (*G. Abell, "Exploration of the Universe," Holt, Rinehart and Winston, Inc., New York, 1964.*)

TABLE 5.2 The wavelengths of selected hydrogen spectral lines in air. (Based on Cox, (ed.), *Allen's Astrophysical Quantities*, Fourth Edition, Springer, New York, 2000.)

Series Name	Symbol	Transition	Wavelength (nm)	Medium
Lyman	Lyα	$2 \leftrightarrow 1$	121.567	vacuum
	Lyβ	$3 \leftrightarrow 1$	102.572	vacuum
	Lyγ	$4 \leftrightarrow 1$	97.254	vacuum
	Ly$_{\text{limit}}$	$\infty \leftrightarrow 1$	91.18	vacuum
Balmer	Hα	$3 \leftrightarrow 2$	656.281	air
	Hβ	$4 \leftrightarrow 2$	486.134	air
	Hγ	$5 \leftrightarrow 2$	434.048	air
	Hδ	$6 \leftrightarrow 2$	410.175	air
	Hϵ	$7 \leftrightarrow 2$	397.007	air
	H$_8$	$8 \leftrightarrow 2$	388.905	air
	H$_{\text{limit}}$	$\infty \leftrightarrow 2$	364.6	air
Paschen	Paα	$4 \leftrightarrow 3$	1875.10	air
	Paβ	$5 \leftrightarrow 3$	1281.81	air
	Paγ	$6 \leftrightarrow 3$	1093.81	air
	Pa$_{\text{limit}}$	$\infty \leftrightarrow 3$	820.4	air

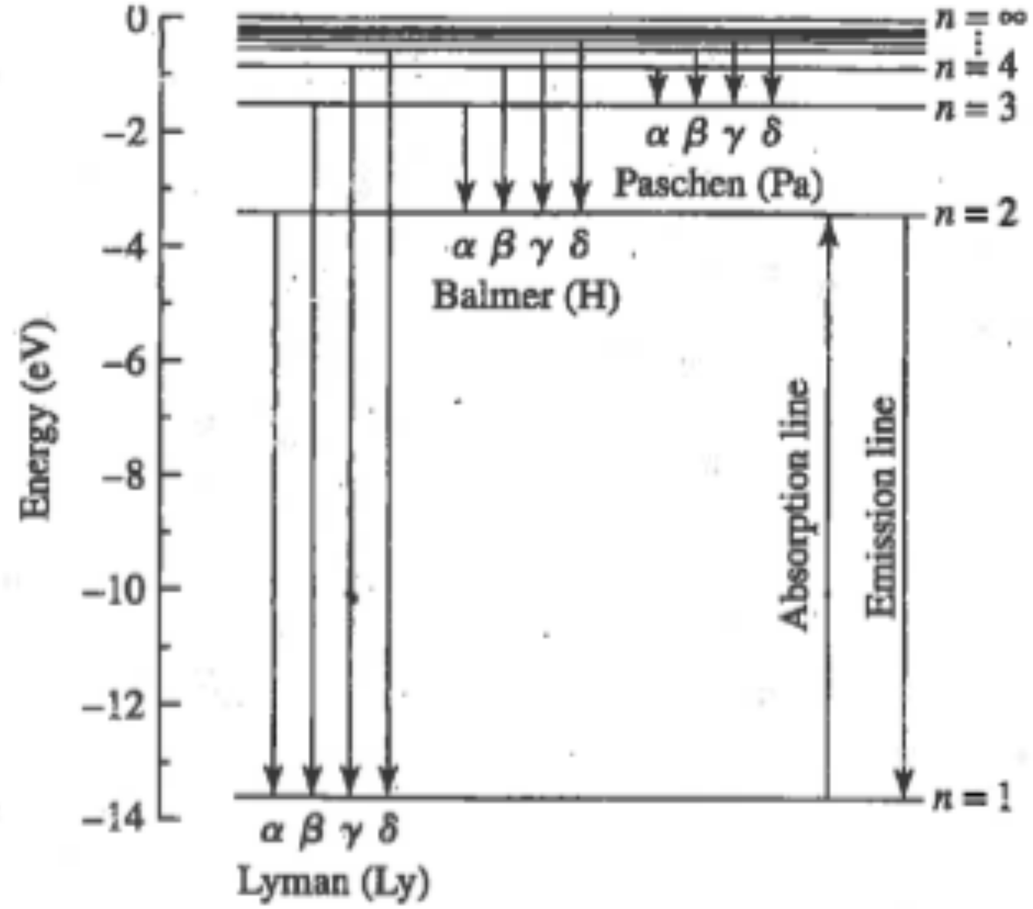

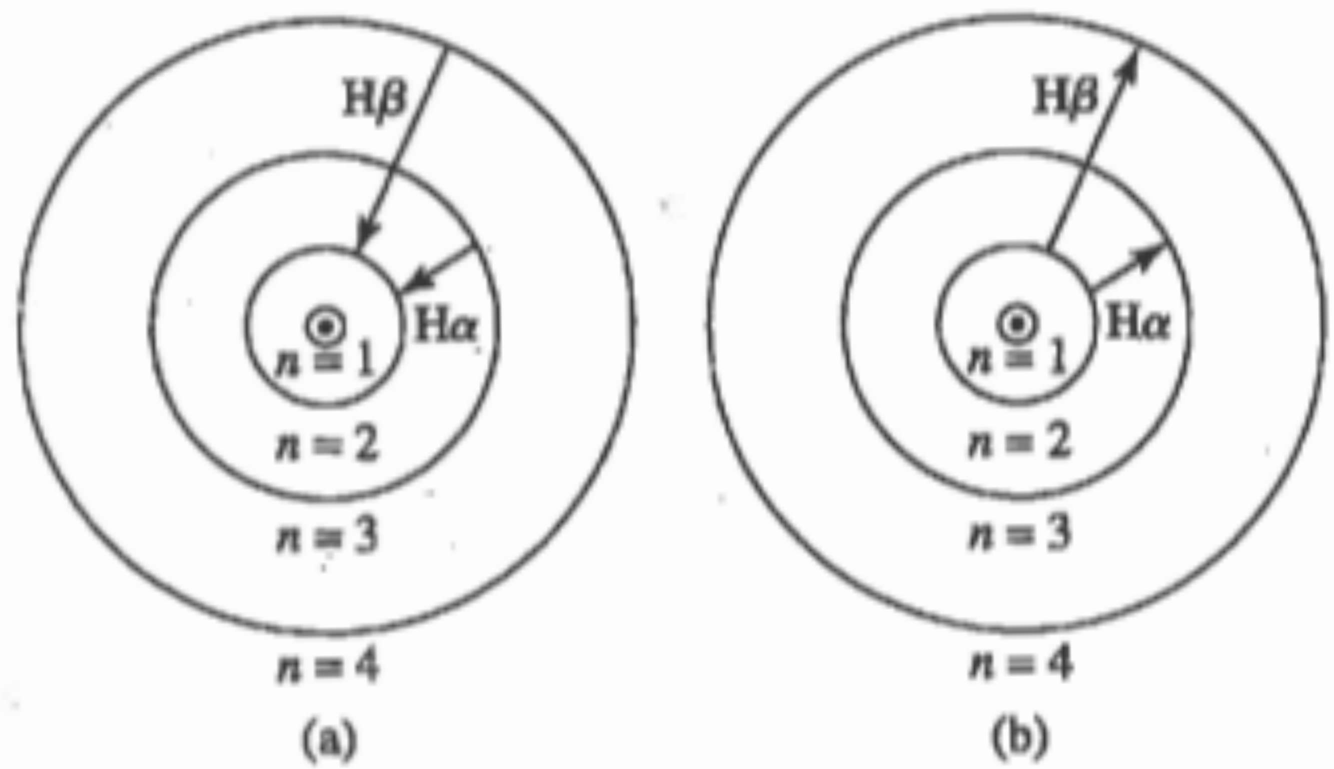

FIGURE 5.6 Balmer lines produced by the Bohr hydrogen atom. (a) Emission lines. (b) Absorpt lines.

TABLE 5.1 Wavelengths of some of the stronger Fraunhofer lines measured in air near sea level. The atomic notation is explained in Section 8.1, and the equivalent width of a spectral line is defined in Section 9.5. The difference in wavelengths of spectral lines when measured in air versus in vacuum are discussed in Example 5.3.1. (Data from Lang, *Astrophysical Formulae*, Third Edition, Springer, New York, 1999.)

Wavelength (nm)	Name	Atom	Equivalent Width (nm)
385.992		Fe I	0.155
388.905		H_8	0.235
393.368	K	Ca II	2.025
396.849	H	Ca II	1.547
404.582		Fe I	0.117
410.175	h, $H\delta$	H I	0.313
422.674	g	Ca I	0.148
434.048	G′, $H\gamma$	H I	0.286
438.356	d	Fe I	0.101
486.134	F, $H\beta$	H I	0.368
516.733	b_4	Mg I	0.065
517.270	b_2	Mg I	0.126
518.362	b_1	Mg I	0.158
588.997	D_2	Na I	0.075
589.594	D_1	Na I	0.056
656.281	C, $H\alpha$	H I	0.402

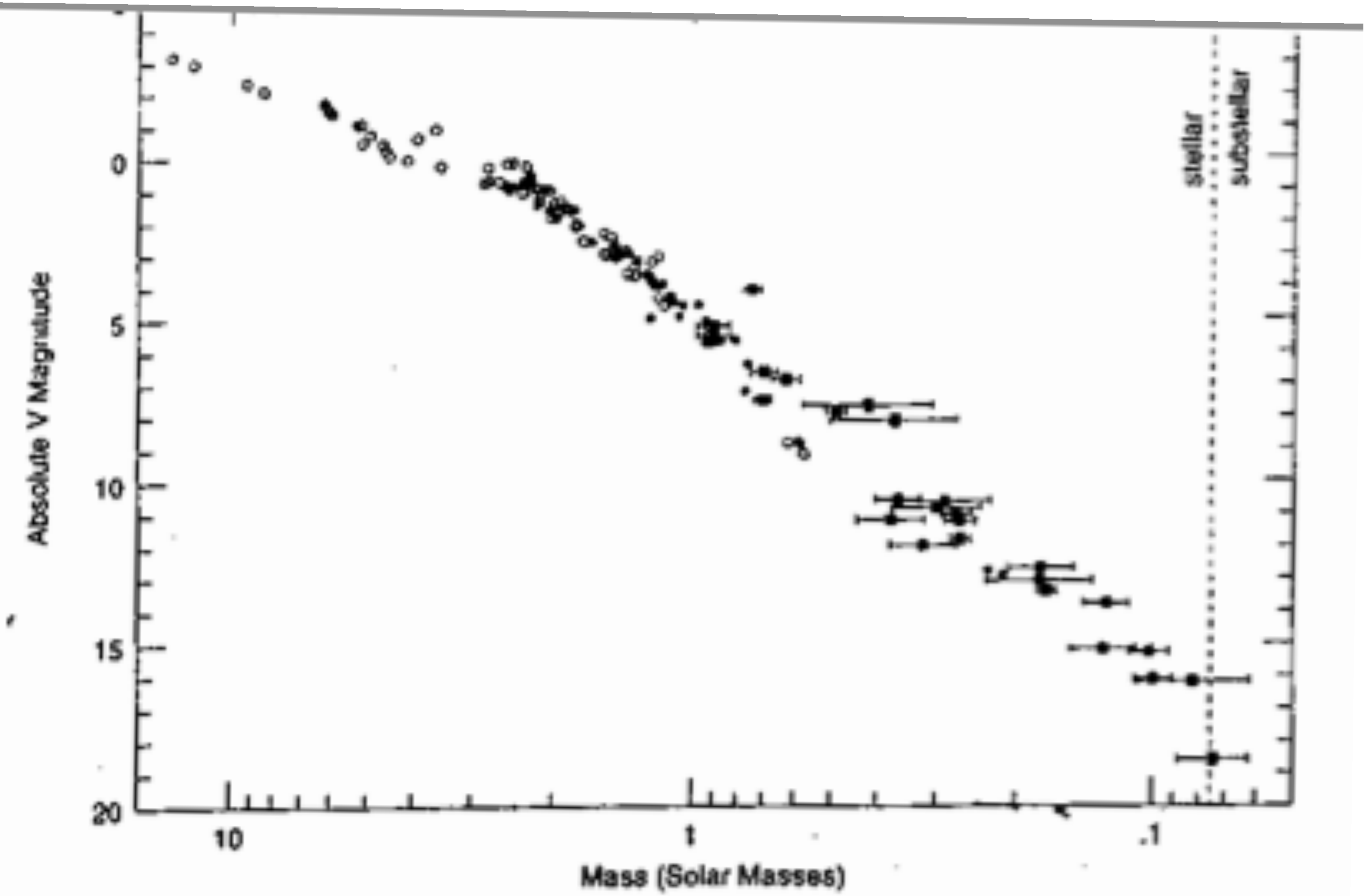

Figure 3.1 Absolute visual magnitude versus mass for components of nearby binary stars. Visual and eclipsing binaries are marked by squares and circles, respectively. [After Latham (1998) courtesy of D. Latham]

Hertzsprung-Russell (HR) diagram

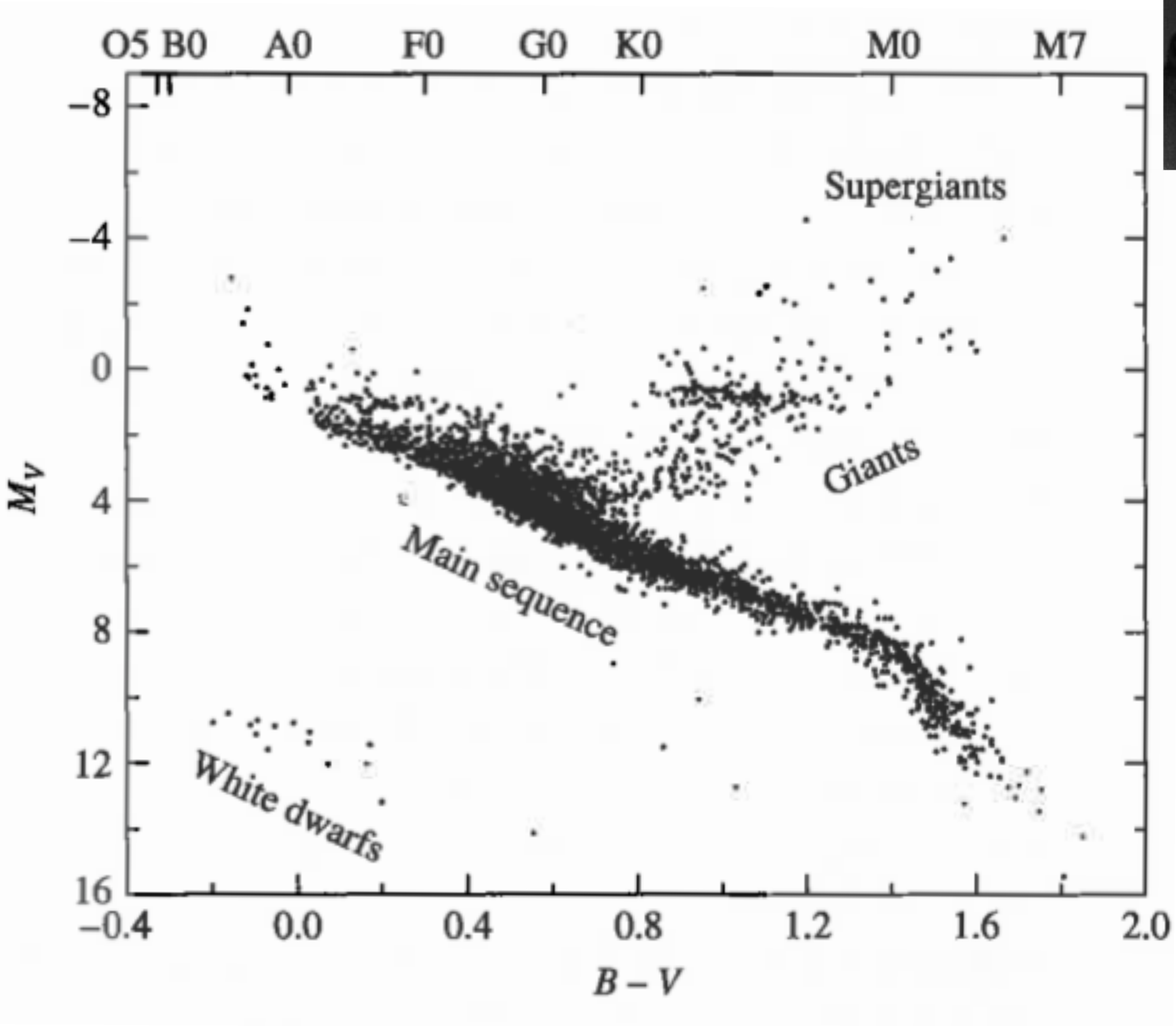

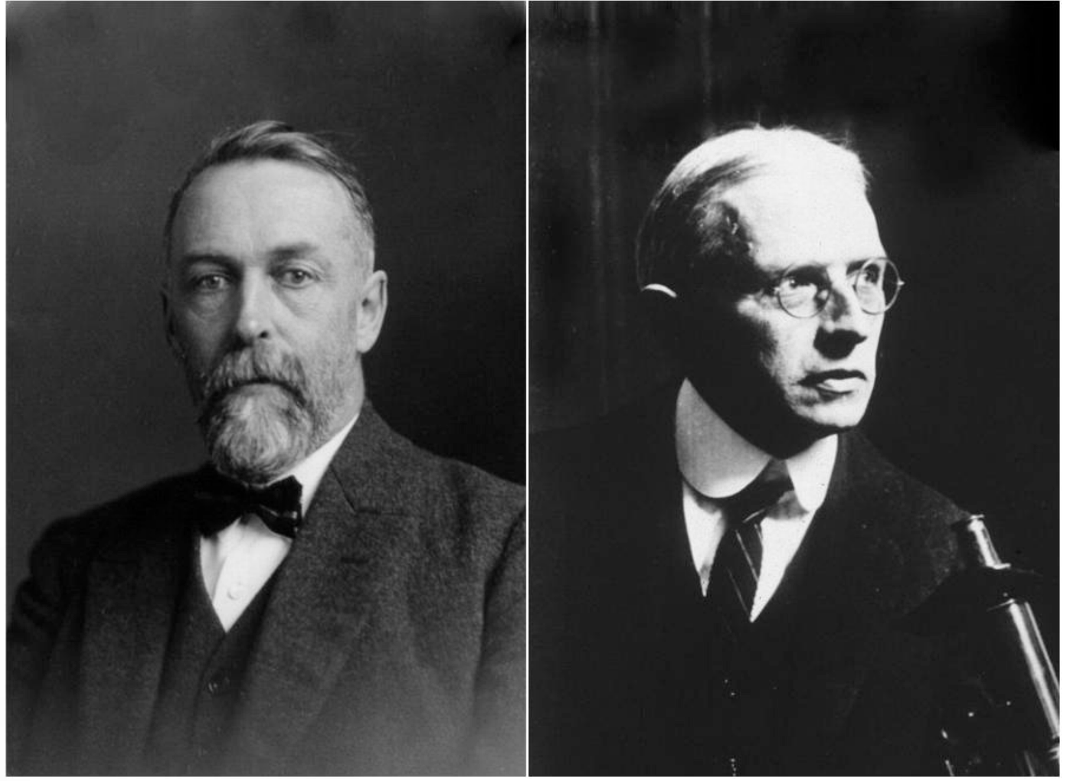

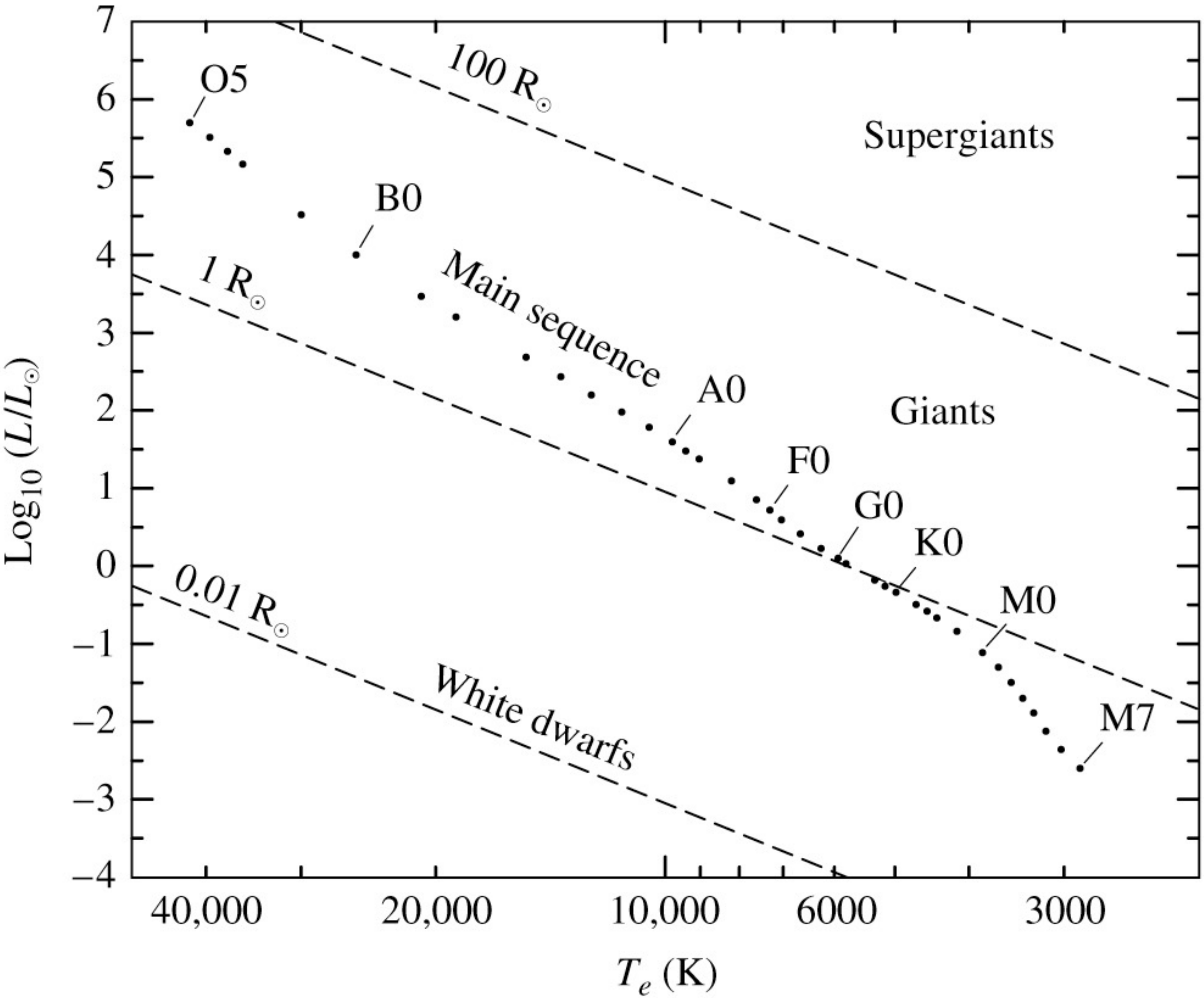
100 $R_\odot$
1 $R_\odot$
0.01 $R_\odot$
Supergiants
Giants
Main sequence
White dwarfs
O5
B0
A0
F0
G0
K0
M0
M7
$\text{Log}_{10}(L/L_\odot)$
7
6
5
4
3
2
1
0
−1
−2
−3
−4
40,000
20,000
10,000
6000
3000
T_e (K)

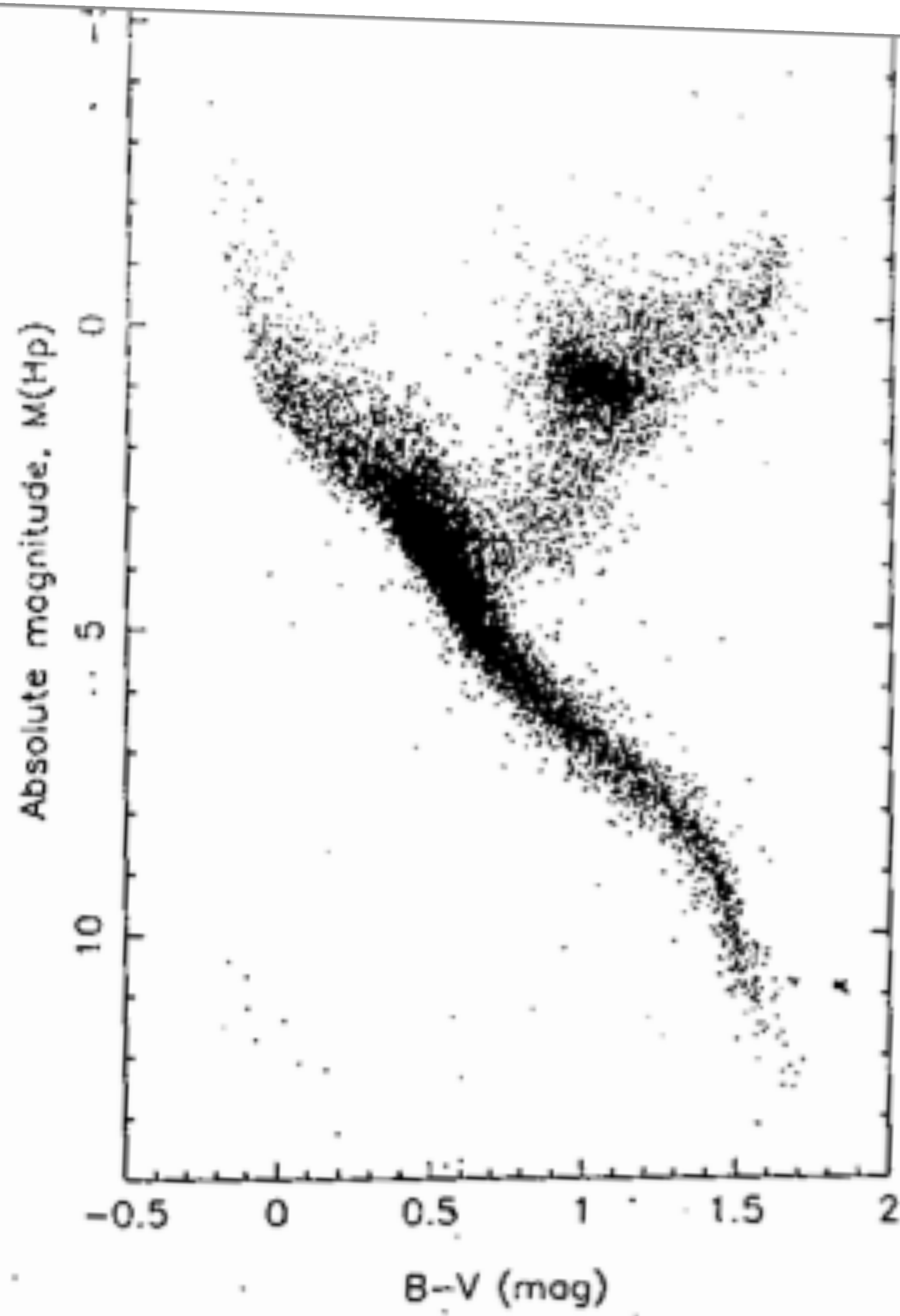

Figure 3.5 The CM-diagram for 10 793 stars with good Hipparcos parallaxes. The great majority of stars fall along the MS that runs diagonally from bottom right to top left. The subgiant, red giant, and white-dwarf sequences are also apparent, as is the red clump. The and WD stars were selected to h parallaxes with errors smaller th 10%, while the giants were chose have parallaxes in error by < 20 [After Perryman *et al.* (1995) co tesy of M. Perryman]

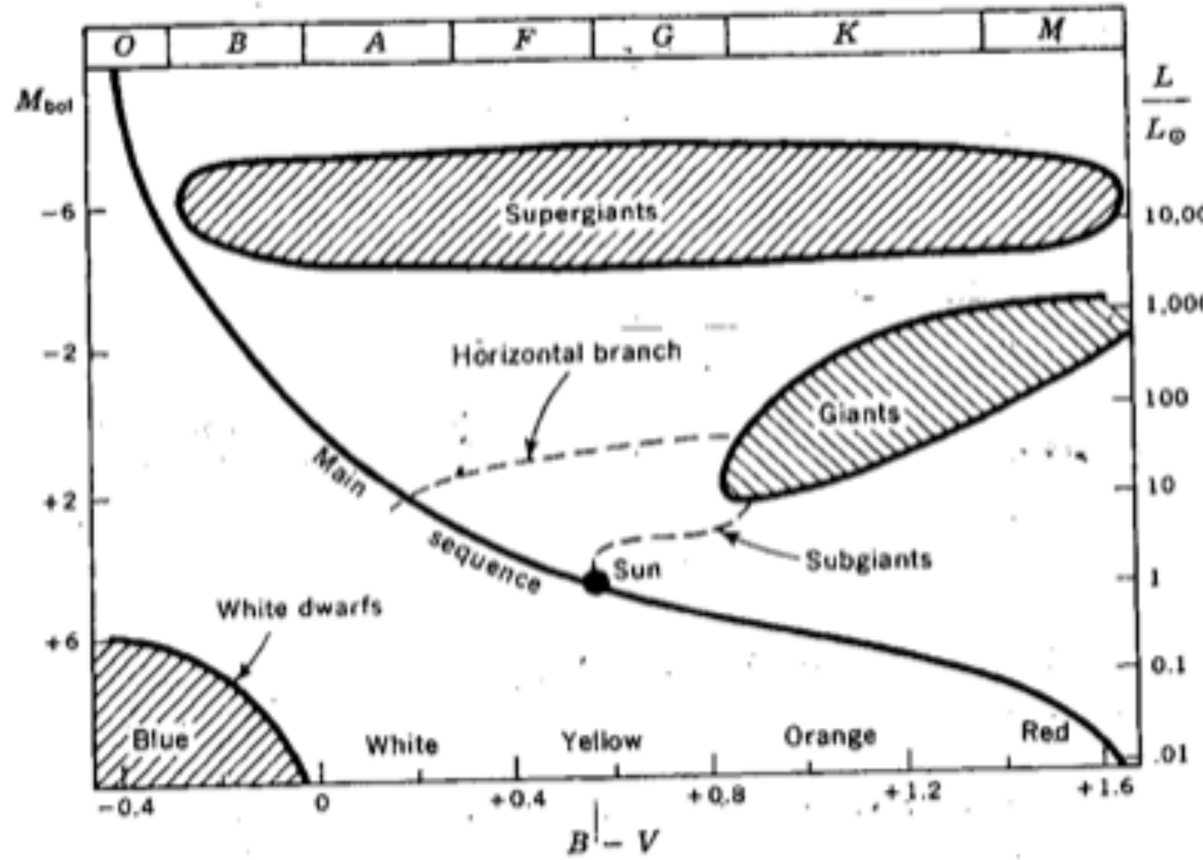

Fig. 1-12 A schematic representation of the heavily populated areas in the H-R diagram. A high percentage of stars lie near the main sequence. The next most populous groups are the white dwarfs and the giants. The subgiant and horizontal branches are conspicuous in those collections of stars having large numbers of giants, e.g., globular clusters.

Table 1-1 The main sequence†

Spectral type	Absolute visual magnitude M_v	Color index $B - V$	Bolometric correction	Effective surface temperature T_e, °K	Color temperature T_c, °K	Absolute bolometric magnitude M_{bol}	Logarithm of luminosity $\log \frac{L}{L_\odot}$
O5	−6.0	−0.45	4.6	35,000	70,000	−10.6	6.13
B0	−3.7	−0.31	3.0	21,000	38,000	−6.7	4.56
B5	−0.9	−0.17	1.6	13,500	23,000	−2.5	2.88
A0	0.7	0.00	0.68	9,700	15,400	0.0	1.88
A5	2.0	0.16	0.30	8,100	11,100	1.7	1.20
F0	2.8	0.30	0.10	7,200	9,000	2.7	0.80
F5	3.8	0.45	0.00	6,500	7,600	3.8	0.37
G0	4.6	0.57	0.03	6,000	6,700	4.6	0.05
G5	5.2	0.70	0.10	5,400	6,000	5.1	−0.15
K0	6.0	0.84	0.20	4,700	5,400	5.8	−0.43
K5	7.4	1.11	0.58	4,000	4,500	6.8	−0.83
M0	8.9	1.39	1.20	3,300	3,800	7.6	−1.15
M5	12.0	1.61	2.1	2,600	3,000	9.8	−2.03

† C. W. Allen, [illegible]

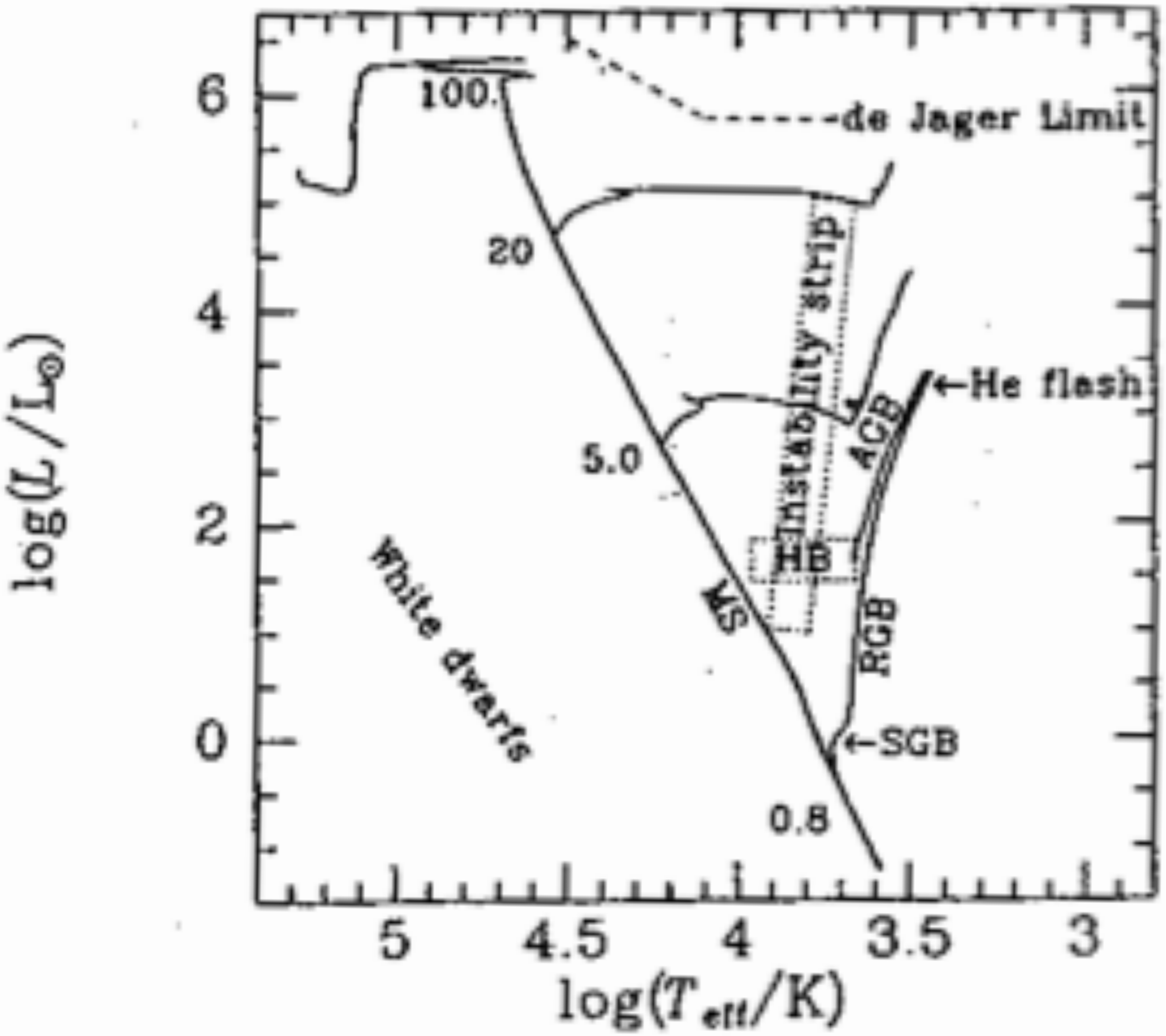

Feature	Physical significance	Remarks
Main sequence (MS)	Core H burning	
Subgiant branch (SGB)	Transition from core to shell H burning	Prominent in globular-cluster CM diagrams
Red giant branch (RGB)	Shell burning of H	For lower-mass stars terminated by He flash
Horizontal branch (HB)	Core He burning	Has characteristic luminosity; color sensitive to metallicity
Red clump (RC)	Stubby red HB formed by more metal-rich stars	Prominent in disk CM diagrams
Asymptotic giant branch (AGB)	Shell He burning	Associated with significant and increasing mass loss; stars often irregular variables
Instability strip	He^+ ionization zone gives rise to regular variables	RR Lyrae and W Virginis stars lie at intersection with HB; Cepheids are massive stars that lie in strip
White-dwarf sequence	Cooling electron-degenerate stars	Blue and faint

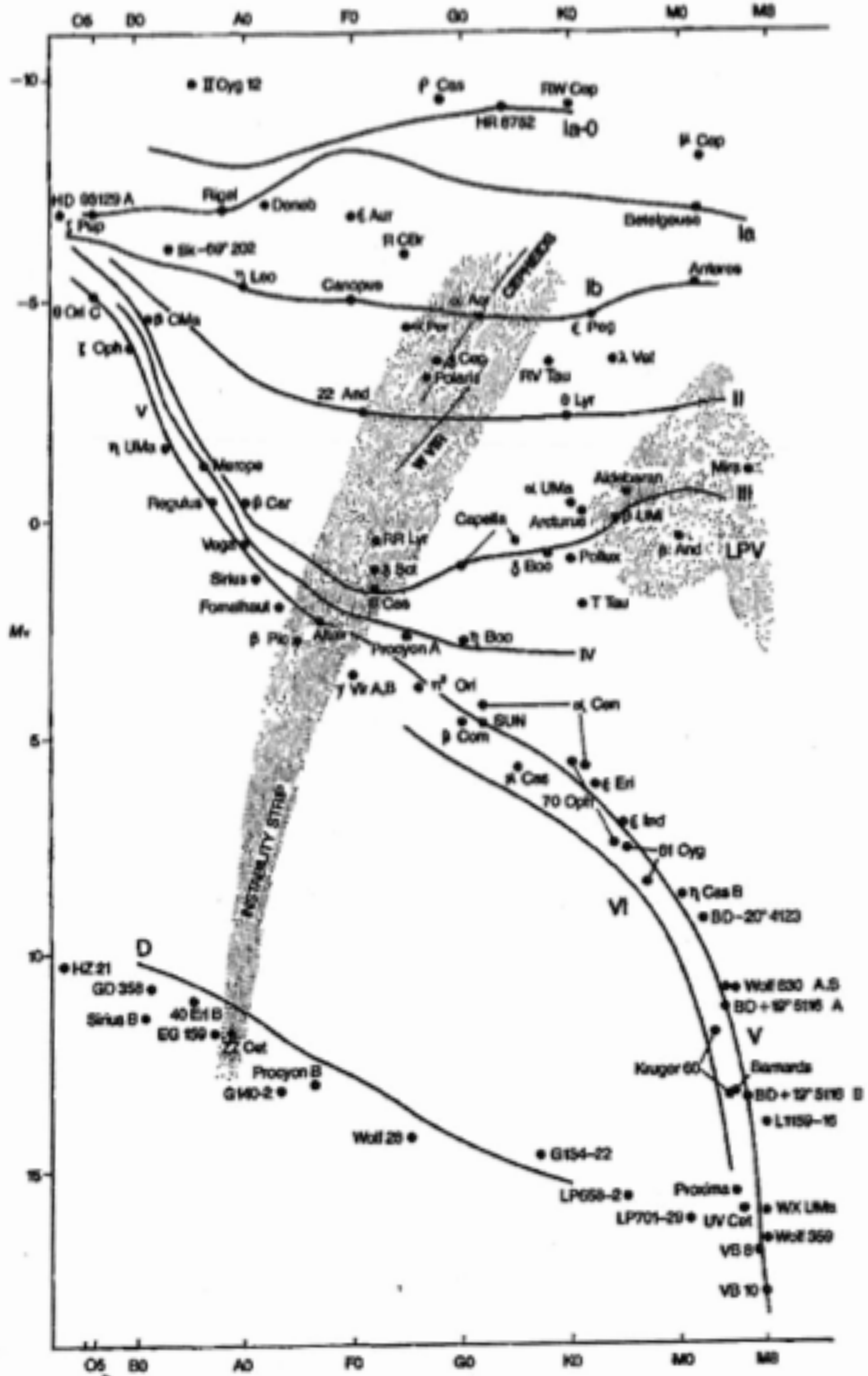

FIGURE 8.16 Luminosity classes on the H–R diagram. (Figure from Kaler, *Stars and Stellar Spectra*, © Cambridge University Press 1989. Reprinted with the permission of Cambridge University Press.)

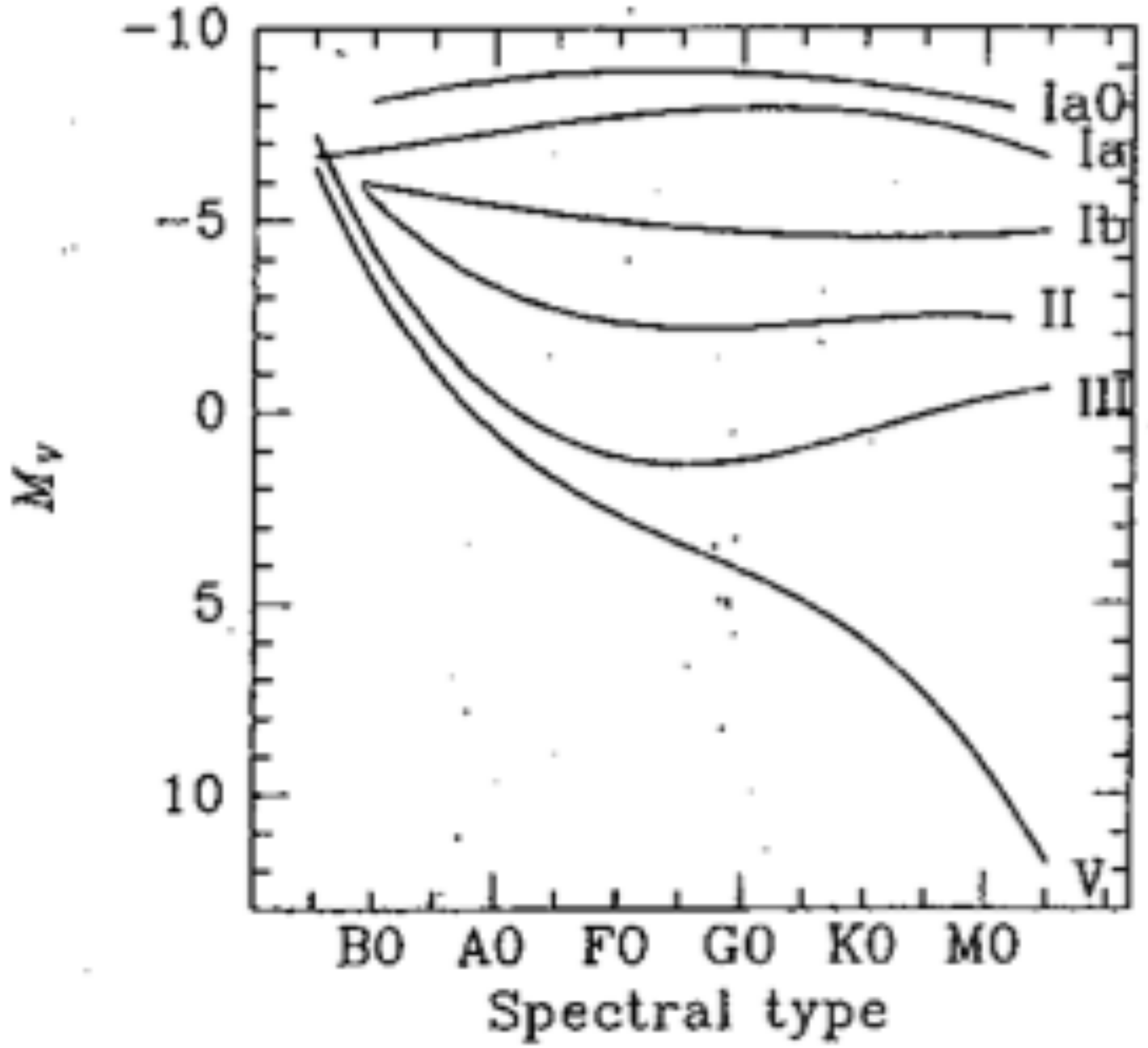

Figure 3.6 Luminosity as a fu[n]
of MK spectral class. The curv[e]
correspond to the luminosity cl[
marked at right.

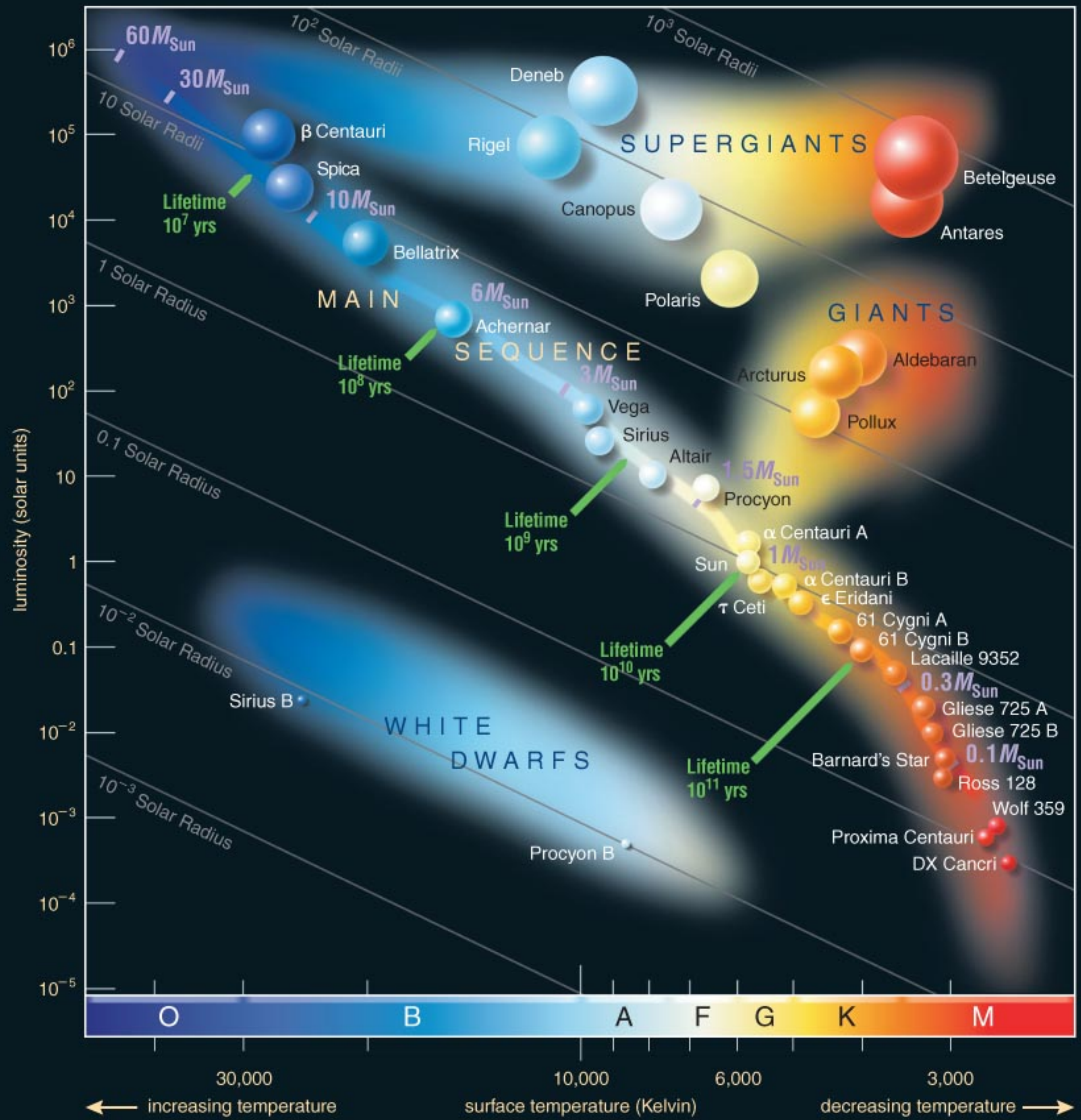
60 MSun
30 MSun
10 MSun
6 MSun
3 MSun
1.5 MSun
1 MSun
0.3 MSun
0.1 MSun
10² Solar Radii
10³ Solar Radii
10 Solar Radii
1 Solar Radius
0.1 Solar Radius
10⁻² Solar Radius
10⁻³ Solar Radius
Deneb
Rigel
β Centauri
Spica
Bellatrix
Achernar
Canopus
Polaris
Betelgeuse
Antares
SUPERGIANTS
GIANTS
Aldebaran
Arcturus
Pollux
MAIN
SEQUENCE
Vega
Sirius
Altair
Procyon
α Centauri A
Sun
α Centauri B
ε Eridani
τ Ceti
61 Cygni A
61 Cygni B
Lacaille 9352
Gliese 725 A
Gliese 725 B
Barnard's Star
Ross 128
Wolf 359
Proxima Centauri
DX Cancri
Lifetime 10⁷ yrs
Lifetime 10⁸ yrs
Lifetime 10⁹ yrs
Lifetime 10¹⁰ yrs
Lifetime 10¹¹ yrs
Sirius B
WHITE
DWARFS
Procyon B
luminosity (solar units)
10⁶
10⁵
10⁴
10³
10²
10
1
0.1
10⁻²
10⁻³
10⁻⁴
10⁻⁵
O
B
A
F
G
K
M
30,000
10,000
6,000
3,000
increasing temperature
surface temperature (Kelvin)
decreasing temperature

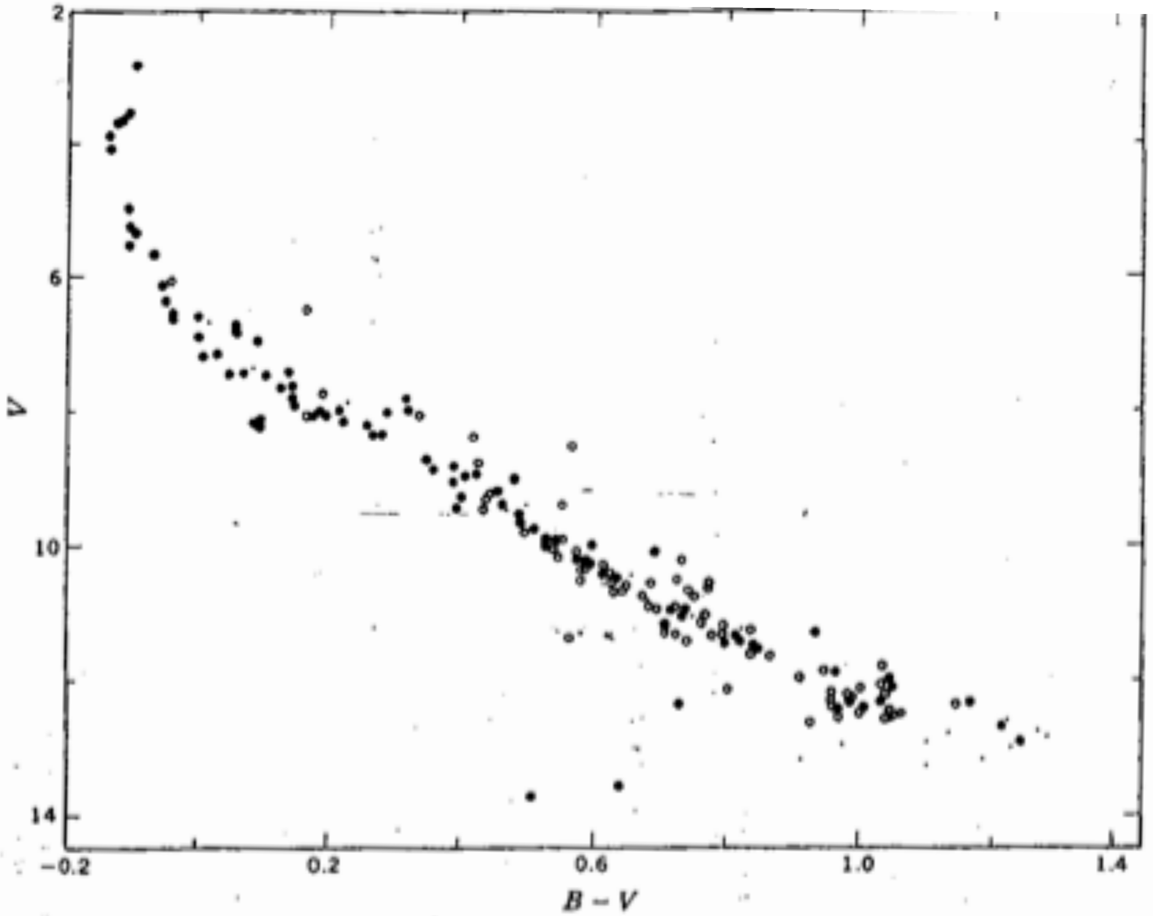

Fig. 1-16 Color-magnitude diagram of the Pleiades with reddening and absorption removed. This young galactic cluster falls very close to the zero-age main sequence, although the upper end appears to have moved rightward. [*After R. I. Mitchell and H. L. Johnson, Astrophys. J.,* **125**:418 (1957). *By permission of The University of Chicago Press. Copyright* 1957 *by The University of Chicago.*]

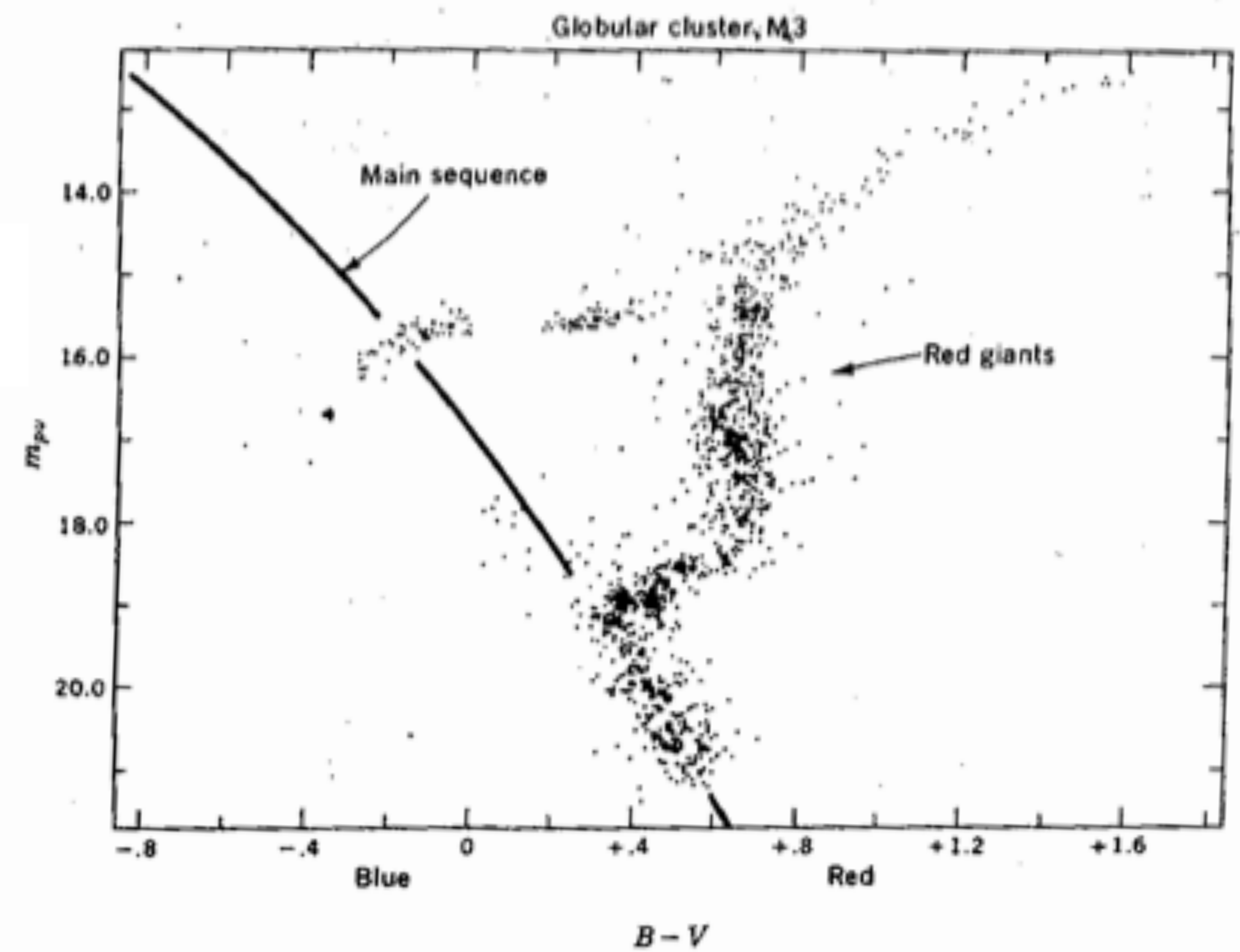

Fig. 1-17 Color-magnitude diagram of the old globular cluster M 3. The main sequence terminates near $B - V \approx 0.3$ and swerves upward along the subgiant branch into the giant region. [*After H. L. Johnson and A. Sandage, Astrophys. J.,* **124**:379 (1956). *By permission of The University of Chicago Press. Copyright* 1956 *by The University of Chicago.*]

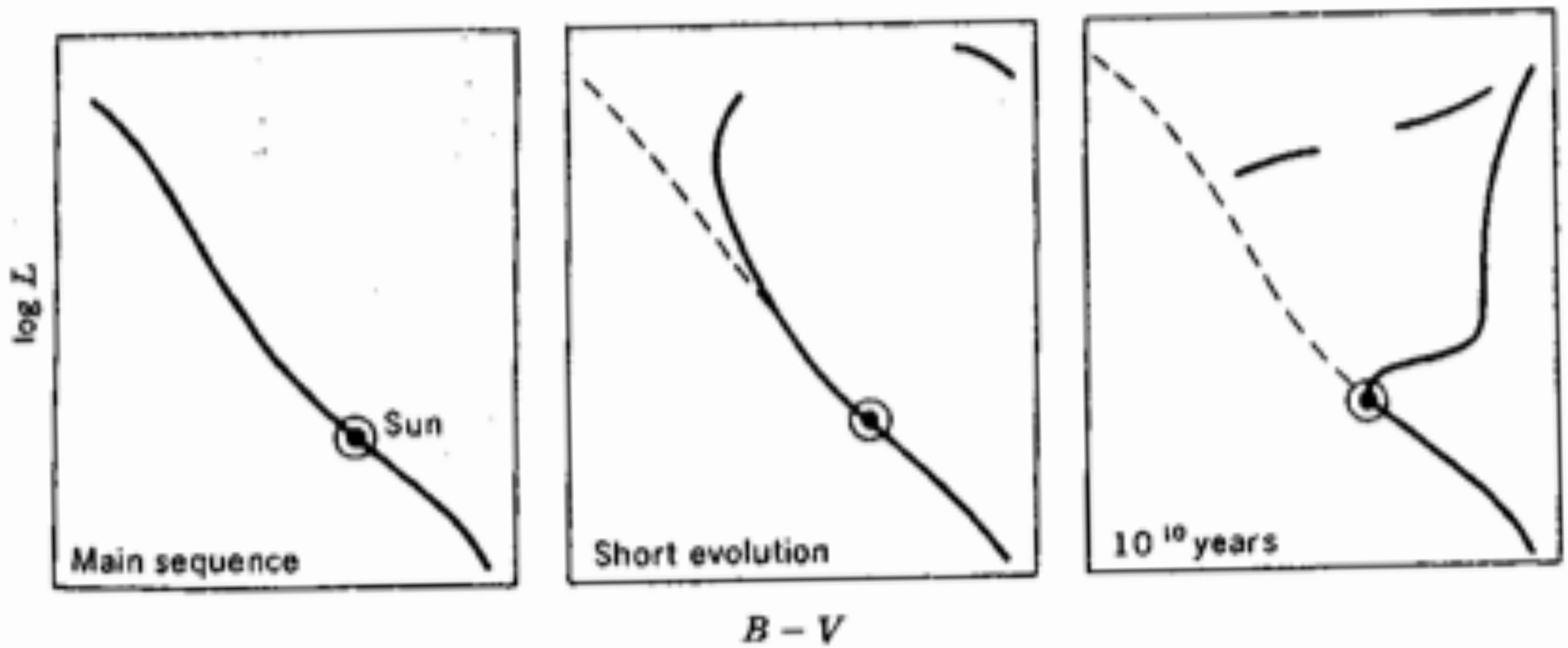

Fig. 1-20 Schematic representation of the H-R diagram of a cluster of stars at three different epochs in its history. After a short period of evolution, say about 10^8 years, the zero-age main sequence has become an evolved main sequence similar to the Pleiades. After a long period of evolution, say about 10^{10} years, the diagram resembles those of the globular clusters. Supergiants and white dwarfs have been omitted from this diagram because their participation is poorly understood.

et al. (1994)]

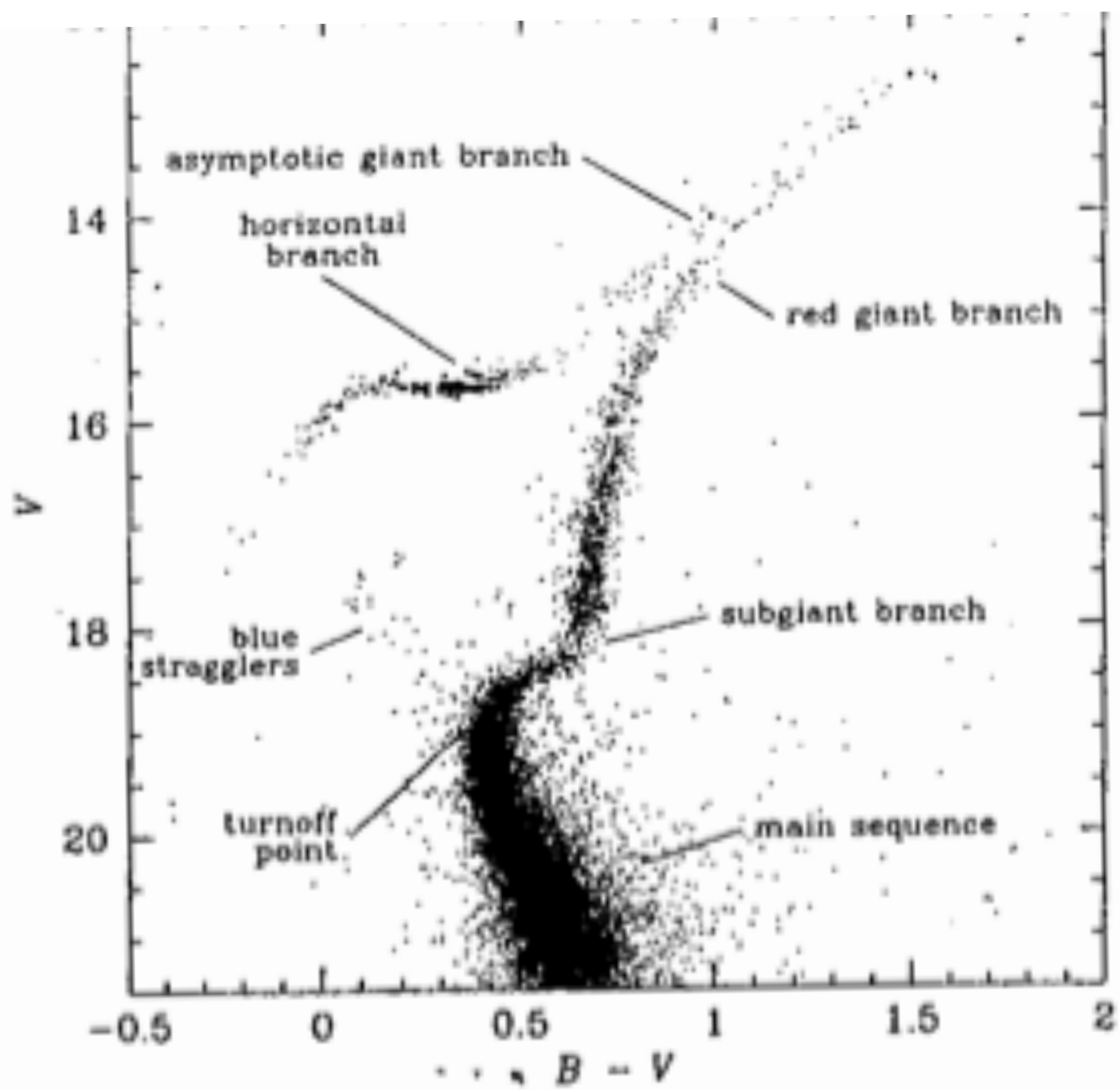

Figure 6.2 The color-magnitude diagram for the globular cluster M3. Known variable stars are shown as open circles, and the principal sequences are annotated. [From data published in Buonanno *et al.* (1994)]

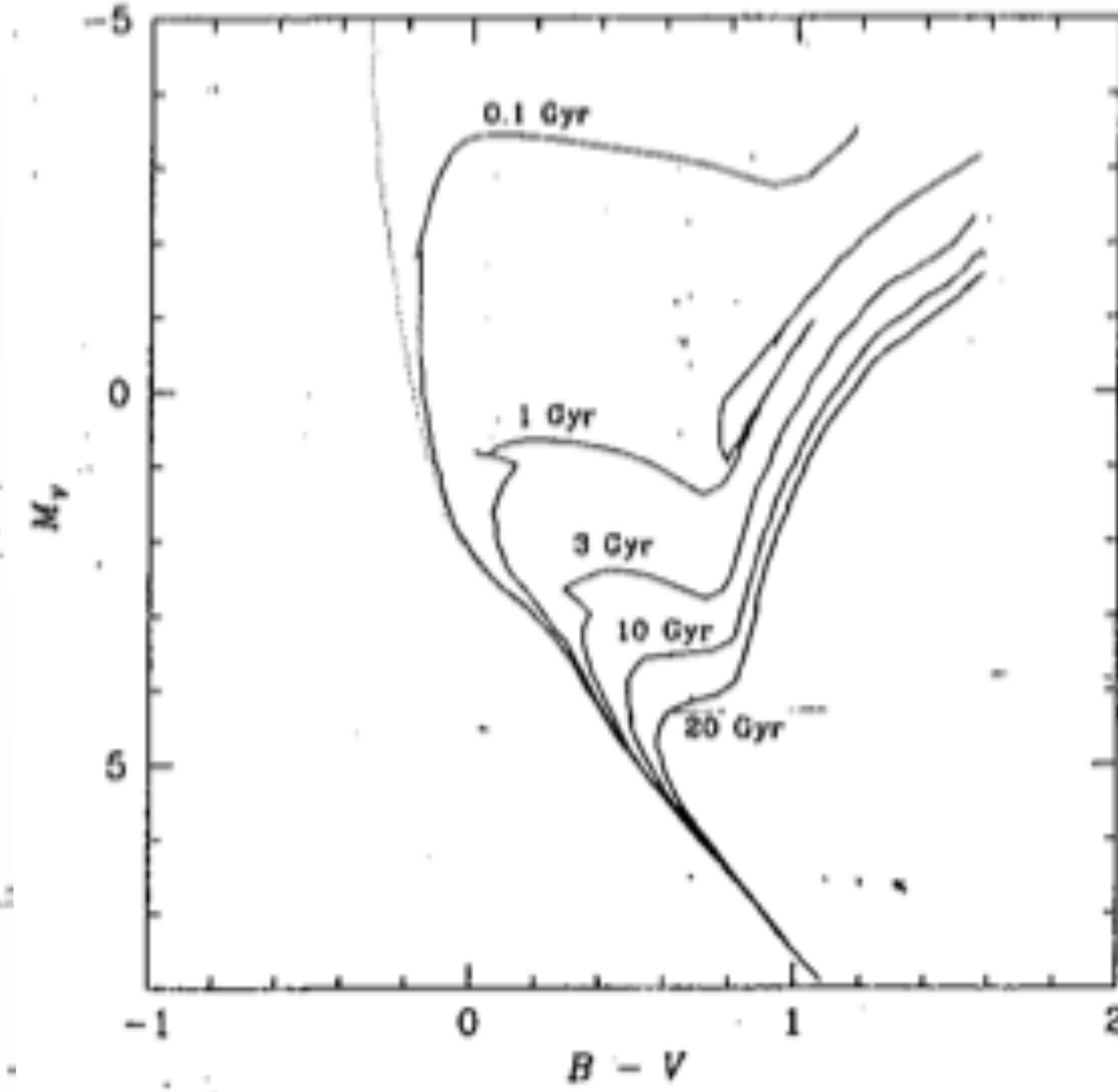

Figure 6.6 Theoretically calculated isochrones showing how a stellar population with $Z = 0.004$, $Y = 0.24$ evolves away from the ZAMS (dotted line) in the CM diagram. Each isochrones is labeled by its age. [From the calculations of Bertelli *et al.* (1994)]

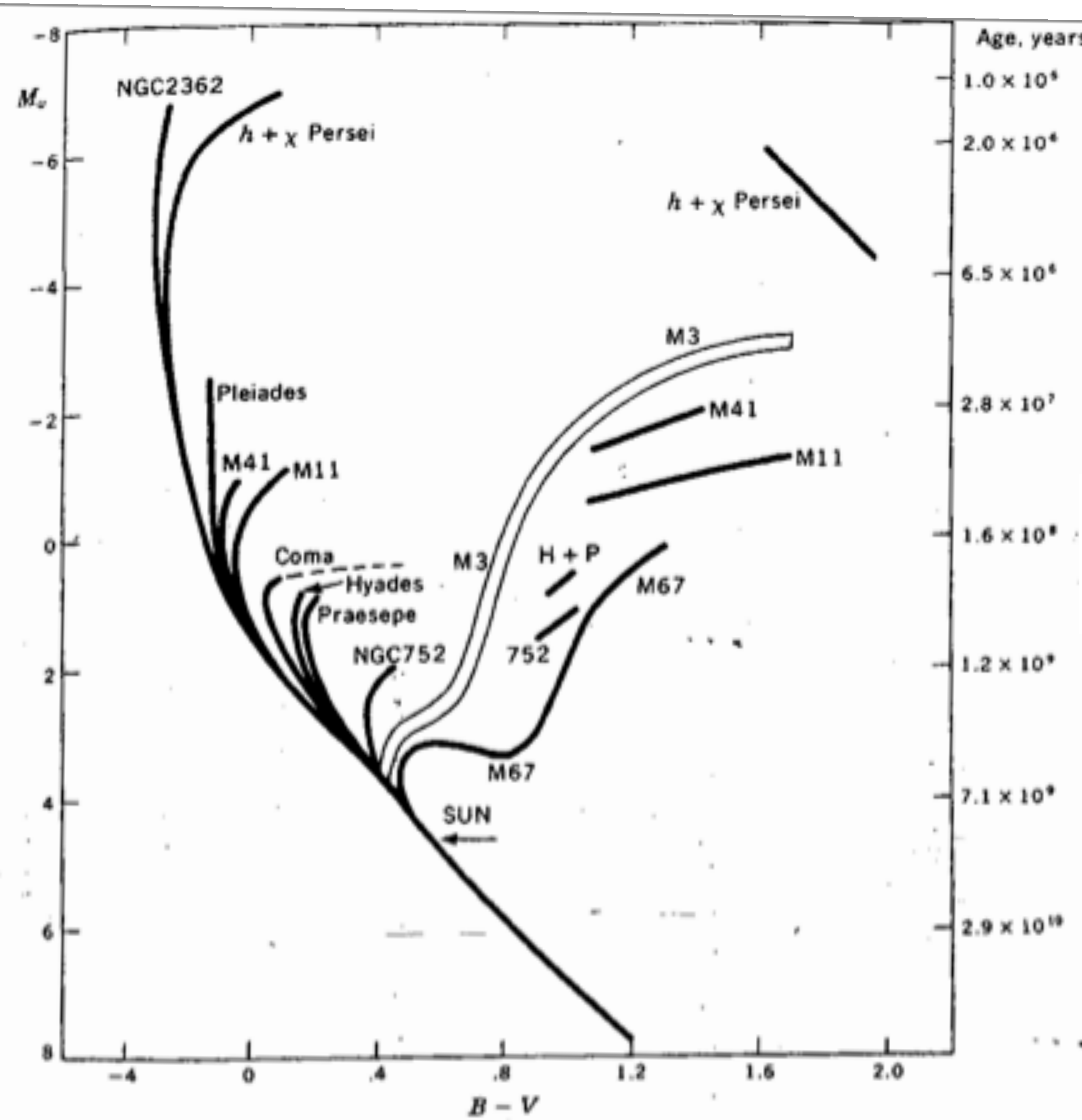

Fig. 1-21 A composite color-magnitude diagram of 10 galactic clusters and 1 globular cluster. Ages corresponding to the various main-sequence termination points are given along the right-hand ordinate. The zero-age main sequence is taken to be the blue envelope of the observed sets of main-sequence stars. Notice the rapidly evolved red giants in $h + \chi$ Persei, which are apparently no more than 2 million years old. Some white dwarfs are known in the Hyades, indicating that it is possible to form them in a few million years, either directly or as the end product of the evolution of upper-main-sequence stars. Curiously enough, the Hyades has no red giants. The oldest galactic cluster, M 67, is older than the sun and has scores of white dwarfs. Many fascinating problems are uncovered in the attempts to interpret the star densities in these diagrams quantitatively. [*After A. Sandage, Astrophys. J.*, **125**:435 (1957). *By permission of The University of Chicago Press. Copyright* 1957 *by The University of Chicago.*]

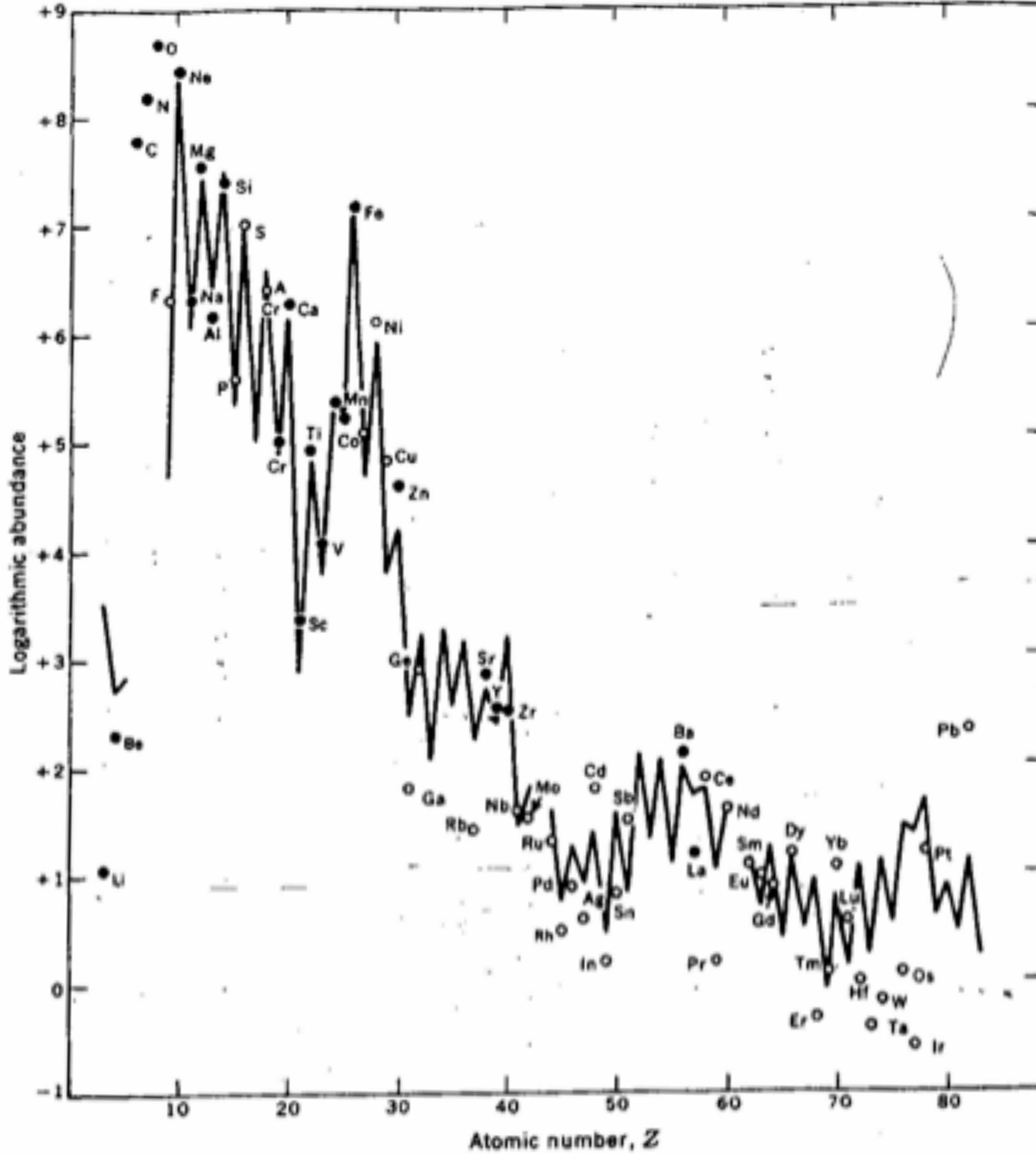

Fig. 1-22 The abundances of the elements in the solar system. The dots represent values obtained from the strengths of absorption lines in the spectrum of the sun, whereas the line represents the historic compilation of Suess and Urey, which was based mainly on chemical evidence from the earth and meteorites. Many of the estimates from both techniques have been improved since 1956, but the general features remain the same. It has been these abundance features which have inspired the nuclear physicists to seek the sets of thermonuclear circumstances that will reproduce this figure in a natural way.

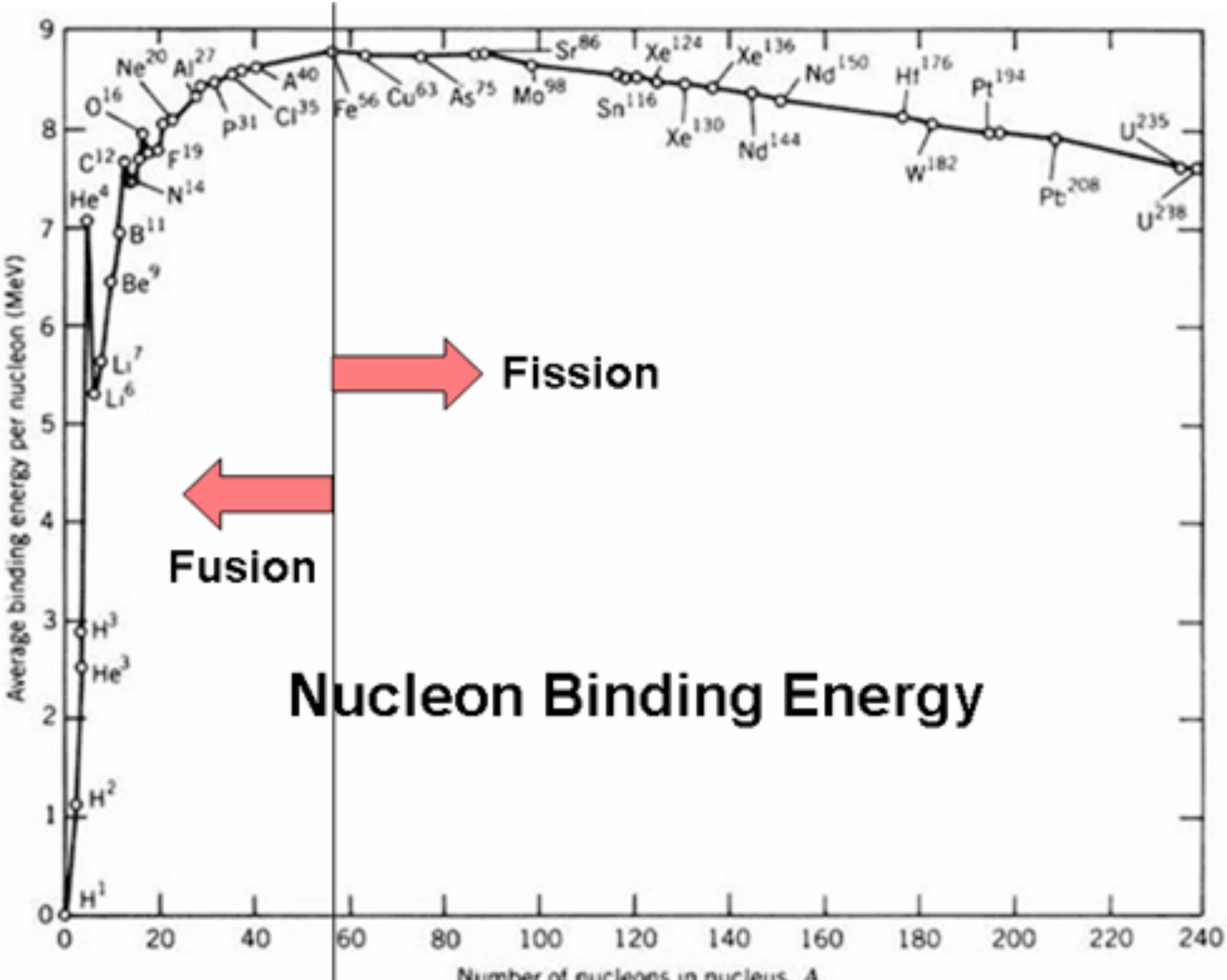

Nucleon Binding Energy
Fission
Fusion
Average binding energy per nucleon (MeV)
Number of nucleons in nucleus, A
H1
H2
He3
H3
Li6
Li7
Be9
B11
He4
C12
N14
F19
O16
Ne20
Al27
P31
Cl35
A40
Fe56
Cu63
As75
Sr86
Mo98
Sn116
Xe124
Xe130
Xe136
Nd144
Nd150
Hf176
W182
Pt194
Pt208
U235
U238